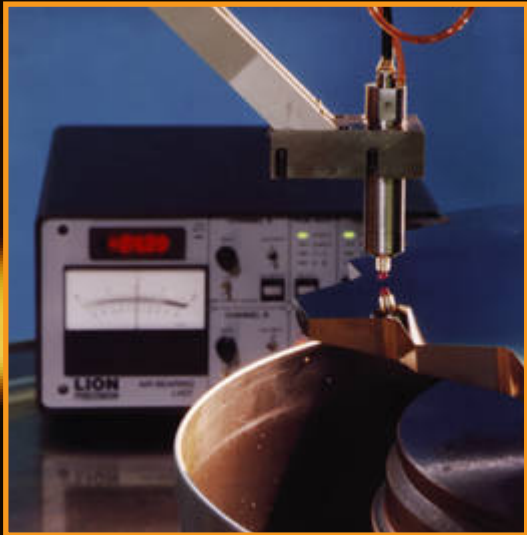
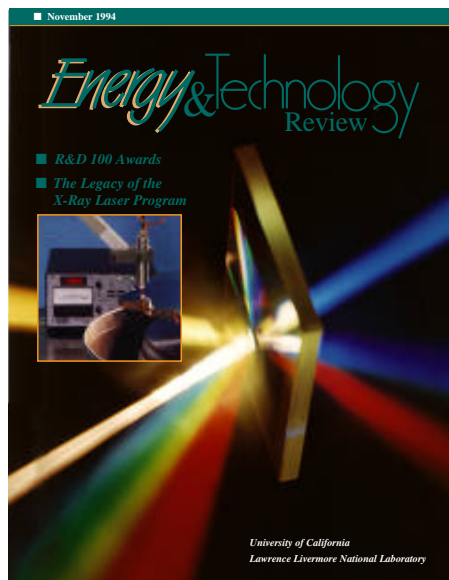


# *Energy* & Technology Review 3/

- *R&D 100 Awards*
- *The Legacy of the X-Ray Laser Program*



*University of California  
Lawrence Livermore National Laboratory*



### About the Cover

The images on this month's cover come from the article, **beginning on p. 1**, about the six R&D 100 Awards won by LLNL employees in 1994. Pictured is a large (15- × 20-centimeter), highly efficient multilayer dielectric grating. It combines the high diffraction efficiency of metal gratings with the damage-resistance of a transparent material particularly useful in the development of high-energy tunable lasers and high-speed supercomputers. The inset pictures an air-bearing linear variable differential transformer (LVDT), a precision measuring device equipped with a high-precision low-noise amplifier. The amplifier improves the resolution of the LVDT to the near-atomic level. Details about these and other award-winning advances in laser technology, fiber-optic communication, and genetic research are provided in our report on the LLNL winners of the 1994 R&D 100 Awards.



Prepared for **DOE** under contract  
No. W-7405-Eng-48

### About the Journal

The Lawrence Livermore National Laboratory, operated by the University of California for the United States Department of Energy, was established in 1952 to do research on nuclear weapons and magnetic fusion energy. Since then, in response to new national needs, we have added other major programs, including technology transfer, laser science (fusion, isotope separation, materials processing), biology and biotechnology, environmental research and remediation, arms control and nonproliferation, advanced defense technology, and applied energy technology. These programs, in turn, require research in basic scientific disciplines, including chemistry and materials science, computing science and technology, engineering, and physics. The Laboratory also carries out a variety of projects for other federal agencies. *Energy and Technology Review* is published monthly to report on unclassified work in all our programs. Please address any correspondence concerning *Energy and Technology Review* (including name and address changes) to Mail Stop L-3, Lawrence Livermore National Laboratory, P.O. Box 808, Livermore, CA 94551, telephone (510) 422-4859, or send electronic mail to [etr-mail@llnl.gov](mailto:etr-mail@llnl.gov).

■ November 1994

**SCIENTIFIC EDITOR**

William A. Bookless

**PUBLICATION EDITOR**

Dean Wheatcraft

**WRITERS**

Kevin Gleason, Robert D. Kirvel,  
Harriet Kroopnick, Carolin Middleton

**DESIGNER**

Kathryn Tinsley

**COMPOSITOR**

Louisa Cardoza

**PROOFREADER**

Al Miguel

This document was prepared as an account of work sponsored by an agency of the United States Government. Neither the United States Government nor the University of California nor any of their employees makes any warranty, expressed or implied, or assumes any legal liability or responsibility for the accuracy, completeness, or usefulness of any information, apparatus, product, or process disclosed or represents that its use would not infringe privately owned rights. Reference herein to any specific commercial product, process, or service by trade name, trademark, manufacturer, or otherwise, does not necessarily constitute or imply its endorsement, recommendation, or favoring by the United States Government or the University of California. The views and opinions of authors expressed herein do not necessarily state or reflect those of the United States Government or the University of California and shall not be used for advertising or product endorsement purposes.

Printed in the United States of America  
Available from  
National Technical Information Service  
U.S. Department of Commerce  
5285 Port Royal Road  
Springfield, Virginia 22161

UCRL-52000-94-11  
Distribution Category UC-700  
November 1994

# Energy & Technology Review

## Feature Articles

### LLNL's 1994 R&D 100 Awards

1

The Laboratory's six 1994 R&D 100 awards acknowledge its contributions to progress in fields ranging from biomedical research, high-speed fiber communication, and ultraprecision engineering, to processes and components that increase the usable power and the versatility of today's lasers.

### Legacy of the X-Ray Laser Program

13

The X-Ray Laser Program, initiated by a laser system for national strategic defense, was the source of several technologies that are now being used for research in diagnostics, plasma physics, biotechnology, medicine, and industrial materials.

## Research Highlights

### Elevated CO<sub>2</sub> Exposure and Tree Growth

22

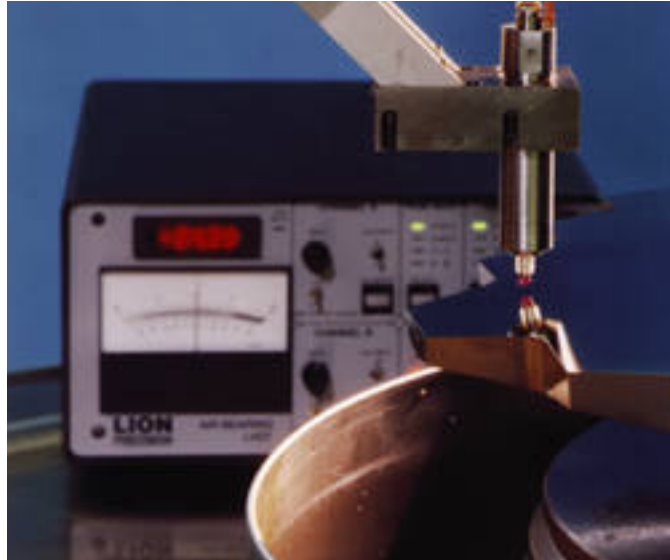
### Meniscus Coating

24

## Abstracts

26

# LLNL's 1994 R&D 100 Awards



*The Laboratory's six 1994 awards demonstrate once again that research derived from defense concerns can contribute civil applications that advance U.S. economic competitiveness and promise improved human well being.*

**E**ACH year *R&D Magazine* selects the 100 most technologically significant products and processes submitted for consideration and honors them with an R&D 100 award. Winners are chosen by the editors of the magazine and a panel of 75 experts in a variety of disciplines. Corporations, government laboratories, private research institutes, and universities throughout the world vie for this “Oscar” of applied research. Past winners include many products that are now a part of everyday life—Polacolor film (1963), the electronic video recorder (1969), antilock brakes (1969), the fax machine (1975), the anticancer drug Taxol (1993). Since the competition began in 1963, the Laboratory has won 50 R&D 100 awards. Among past winners are the

process for the diamond turning of optics (1978), the precision-engineering research lathe (1986), ultralow-density silica aerogel (1990), and the hard x-ray lens (1991).

The R&D 100 judges look for products or processes that promise to change people's lives, such as by significantly improving the environment, health care, or security. In 1994, the Laboratory received six R&D 100 awards. Three of them contribute to advances in laser technology:

- Our new multilayer dielectric diffraction gratings free lasers from the limitations imposed on them by conventional metallic gratings currently in use.
- Our methods for rapidly growing high-quality crystals will change the

economics of using crystals in lasers of all sizes and powers, especially solid-state, which are especially versatile by virtue of combining high power and small size.

- Our doping of several varieties of apatite crystals with ytterbium has achieved significant increases in the energy storage efficiency of diode lasers.

Each of these three inventions also contributes significantly to research in inertial confinement fusion, which promises someday to be a major source of energy for civil uses.

The other award winners are in the fields of high-precision measurement, silicon microbench technology, and genetic research:

- We have advanced the limits of high-precision metrology by developing

an amplifier for use with sensors that measure surface irregularities. This amplifier offers 30 to 40 times better resolution than other high-precision metrology devices using a similar sensor.

- As ever-finer diameters of fibers are used to increase the speed of fiber-optic communication, we have developed a method of achieving the required submicrometer accuracies of component alignment at 10 to 20 times less cost than that of current methods.
- Finally, our chromosome-specific DNA probes allow us to identify chromosomes of the laboratory mouse 60 times faster than the standard chemical staining or banding method.

The analysis of "painted" chromosomes does not require highly skilled personnel, so the savings in personnel cost combined with the increased speed yield a 200-fold increase in efficiency. The many applications of chromosome "painting" include several related to cancer and birth defects, gene mapping, and, perhaps most immediately significant, testing new drugs for safety.

### Efficient Multilayer Dielectric Gratings

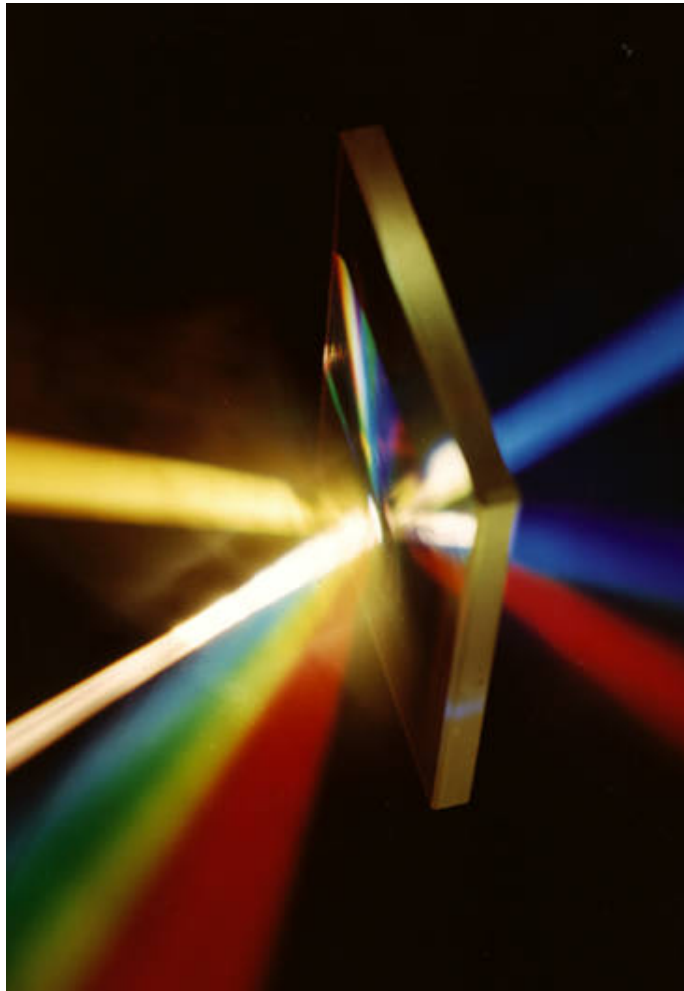
Diffraction gratings have long been used to disperse light into constituent colors, or wavelengths, for

spectroscopic applications. These gratings are finding new uses with high-power lasers. Indeed, their dispersive properties are making possible new classes of lasers: because matched grating pairs can stretch or compress a pulse, grating-pair pulse compressors allow pulses of hitherto unsurpassed intensities to be achieved. However, to accomplish this compression, the gratings must be able to withstand high intensities. Traditional reflection gratings use metallic corrugations to form the needed periodic grooves. They achieve a highly reflective surface by means of the high conductivity of the metal. Heating of conduction electrons, however, renders the surface susceptible to damage at fluences of around  $0.5 \text{ J/cm}^2$ . This low threshold for damage has impeded attempts to develop high-power lasers.

Metallic surfaces are only one means of reflecting light. It has long been known that multiple layers of thin dielectric films act as a highly reflecting structure (because each layer introduces a quarter of a wave of phase retardation). When produced with proper care, these can have high thresholds for laser-induced damage, an order of magnitude higher than those of metallic gratings. In 1991, we proposed that such multilayer dielectric stacks, with a periodic groove structure, could serve as a highly efficient reflection grating. A grating constructed entirely from dielectric material should combine the high damage threshold of transparent material with the high diffraction efficiency hitherto exclusive to metal gratings.

We have demonstrated that such multilayer dielectric gratings can be produced, that they can reflect selected wavelength bands with high efficiency, and that they can be made in large sizes while maintaining high quality wavefronts. The construction of these

**Figure 1. A multilayer dielectric diffraction grating designed to reflect yellow light, diffract broadband visible radiation (bottom left), eliminate all green and yellow light in the transmitted diffracted beam (at right), and transmit blue-green light. The grating pictured is 15 × 20 centimeters.**



gratings has required that several technologies be integrated in order to create the multilayer dielectric stack, to form a periodic latent image pattern in a two-beam interferometer, and to develop this image and transfer the pattern into a permanent grating.

Multilayer dielectric gratings have several novel properties that offer unique opportunities for new applications:

- With their high damage threshold, our dielectric gratings make possible the construction of grating-pair compressors for kilojoule laser pulses that would destroy metallic gratings.
- For any given wavelength, polarization, and angle of incidence, grating efficiency depends on the phase retardation properties of the multilayer stack, the depth and shape of the grating grooves, and the angle of incidence of the radiation. Adjustments of these properties during manufacture make it possible to control the distribution of energy between reflected, transmitted, and diffracted beams.
- The wavelength discrimination of the multilayer stack makes it possible to build gratings that transmit or reflect light with high efficiency within a narrow optical wavelength bandwidth. A grating can be designed to have nearly any desired efficiency and bandwidth.
- Large, high-efficiency gratings, well beyond the 20 × 30 cm size of conventional metallic gratings, are possible with this new technology. Meter-scale gratings, which are now possible, are a key enabling technology for developing high-energy (1000-TW) picosecond-pulse lasers. The laser program at LLNL is planning to use this technology in constructing the world's first 1000-TW laser.

These highly efficient multilayer dielectric gratings create the opportunity for the development of new products. They may replace the metallic gratings

that have become obsolete in many current applications. Broadband solid-state lasers, for example, have become increasingly important devices because their very high output energies make them well suited for compact and reliable systems. However, the full potential of these lasers cannot be realized while they rely on metallic gratings. Dielectric gratings, with their greater threshold for laser-induced damage, will allow the development of high-power tunable narrowband lasers that efficiently extract energy from broadband solid-state materials.

Our new gratings have numerous commercial applications derived from their damage resistance and their ability to act as narrow- or broadband filters or reflectors. When used in commercial laser pulse-compression systems, these designs can substantially reduce grating size over those now used, with proportional cost savings.

The optical selectivity of these gratings will find immediate use in high-contrast spectrometers, which now use multiple conventional gratings to achieve the often-required spectral discrimination to one part per million. Dielectric gratings can be excellent discrimination filters; they can be designed to reflect undesirable narrow-line optical radiation, such as laser radiation, while transmitting most other frequencies. This property may make them valuable on the battlefield, where lasers are increasingly present in weapons and guidance systems. A multilayer grating could transmit visible radiation and diffract unwanted laser radiation with great efficiency.

Because they control distribution of energy between the specularly reflected, transmitted, and diffracted beams (see [Figure 1](#)), gratings can act as selective beam splitters in optical switches and distribution systems. The small-scale, high-energy tunable lasers made possible by these gratings should find numerous uses in such

areas as remote sensing and biochemical or biomedical diagnostics.

*This work was done in cooperation with Hughes Electrooptic Systems in El Segundo, California.*

**For further information contact  
Michael D. Perry (510) 423-4915 or  
Robert Boyd (510) 422-6224.**

## Growing High-Quality KDP Crystals Quickly

Crystals are essential materials in advanced scientific tools and applications, such as portable, high-power solid-state lasers operating in the visible and ultraviolet spectral regions; remote sensing infrared detection systems; engineered molecules for the pharmaceutical industry; and inertial confinement fusion lasers. High-power lasers for fusion require very large, high-quality crystals of potassium dihydrogen phosphate (KDP) and its deuterated analog DKDP for experiments in fusion.

Conventional techniques for growing crystals from solution are slow and inherently unreliable. (Briefly, crystals are grown from a seed, or "starter," crystal that is submerged in a melt or solution containing the same material; the final growth, having the same atomic structure as the seed, is called the boule.) Growth rates for conventionally grown KDP, for example, are about 1 mm/day. Because of a high density of dislocations, or defects, in the material near the seed crystal in KDP, the quality is low; and because the seed defects propagate into the final boule, a substantial fraction of the boule is of low quality. A large percentage of crystals that have taken a long time to grow are, in the end, useless for their intended purpose.

We have developed a process for growing crystals from solution that is appreciably faster than current commercial processes and produces exceptionally high yields of high-quality crystals. Using our rapid-growth method, we have grown both KDP and DKDP crystals up to  $15 \times 15 \text{ cm}^2$  in cross section at rates of 5 to 40 mm/day; that is, 5 to 40 times the rate of conventional methods. Our process uses a small "point" seed and produces only a small number of dislocations. As a result, even material near the seed is of high quality. By saving growth time and reducing waste, our method reduces the cost of crystals. **Figure 2** shows two KDP crystals, one grown conventionally in six weeks and the other grown by our process in two and a half days.

Our process relies on pretreatment of solutions using high temperature and ultrafiltration. This process destroys any small crystal nuclei that might be present in the solution and allows it to be highly supersaturated without

spontaneous crystallization. We use a crystallizer (the process vessel in which the supersaturated solution is brought to a solid crystal state) that eliminates sources of undesired crystal nuclei (spurious nucleation) during growth. Of secondary importance to the method are the technique for holding the seed, the temperature profile during growth, and the hydrodynamic regime. The two major advantages of this process over conventional growth methods—high growth rate and potentially high yields—dramatically reduce labor costs and therefore total cost.

At LLNL we submit crystals to characterization tests while they are growing so that at any stage we know such characteristics as their optical homogeneity, transmitted wavefront distortion, and susceptibility to laser-induced damage. Such methods as x-ray topography and microbeam chemical analysis allow us to trace the optical distortions to structural defects and compositional inhomogeneities. Indeed, atomic force microscopy

enables us to observe crystal growth and defect generation at the nanometer level, giving us direct information about how surface morphology during growth depends on growth conditions and the structure of defects. The information provided by these characterization techniques is used to optimize the growth process iteratively.

Having investigated crystals grown by both conventional and rapid-growth methods, we have demonstrated that the quality of the crystals is not a function of growth rate. Rather, it depends on solution purity, hydrodynamics (the flow geometry of the solution), and the conditions during seed regeneration.

Our process is a significant technical advance in the field of crystal growth. Many crystals that are expensive and difficult to grow will soon become readily available as will others that previously could not be grown to usefully large sizes. Extremely large crystals ( $10,000\text{-}100,000 \text{ cm}^3$ ) for applications such as laser fusion take as long as 2 years to grow and involve great risk of failure. These will be grown in 1 to 2 months and present greater odds of being of sufficient quality. In short, our process is revolutionizing the way solution-based crystals are grown.

Moreover, because it is based on general principles, this technique is applicable to a wide variety of crystal systems. Our process can be used for growing other water-soluble crystals, and we have grown numerous varieties. In all cases, they grow about ten times faster than their conventional counterparts.

The general principles also apply to the stabilization of supersaturated solutions at any temperature or pressure. Modifications of this process should thus be useful with hydro-

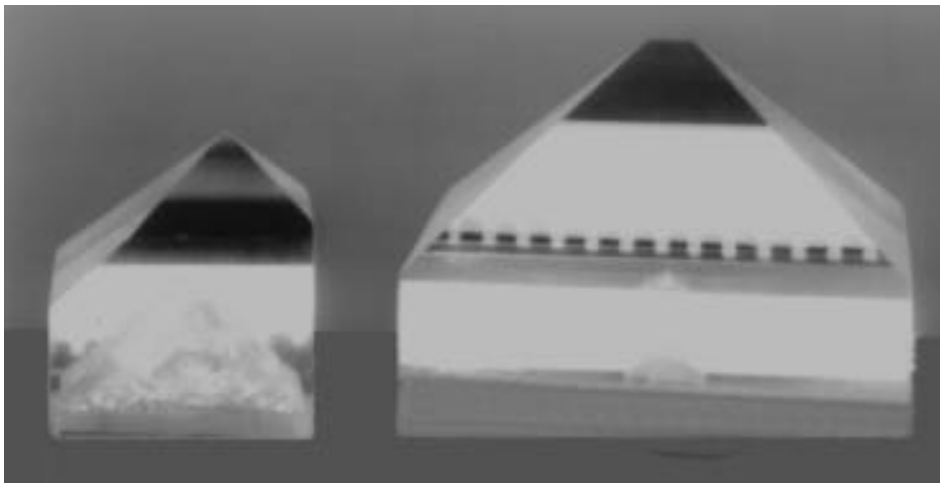


**Figure 2.** The KDP crystal on the left took six weeks to grow by a conventional method; the large, high-quality KDP crystal on the right is approximately 10.5 cm on a side and was grown in only two and a half days using our method.

thermally grown crystals, like quartz, and flux-based systems, such as potassium titanyl phosphate (KTP), lithium borate (LBO), and beta beryllium borate (BBO)—three important optical materials whose application has been limited by the size and quality of currently available crystals. Because such crystals are critical to a number of high-power, visible-to-ultraviolet solid-state laser configurations, wide availability of inexpensive, high-quality crystals would make such configurations possible.

Technologies are limited by the quality and capacity of the best available materials. By improving the solutions, our method removes some limitations. As a national laboratory, we are looking for ways to improve the productivity and competitiveness of U.S. businesses. LLNL has a long-standing relationship with U.S. crystal growth companies, and we are formally involved in commercializing this technology for the rapid growth of KDP and its analogs as well as other crystals.

*This work was done in cooperation with Moscow State University, Moscow, Russia.*

**For further information contact  
James De Yoreo (510) 423-4240.**

## Ytterbium-Doped Apatite Laser Crystals

We have developed a new class of laser materials whose special properties make them a particularly useful invention at a point when laser diode pump sources are becoming a mature technology. Laser diodes are highly efficient and reliable, are rapidly falling in price, and are, therefore, becoming more common in laser systems. Our challenge was to find new laser materials that could fully

exploit the advantages of diode lasers as optical pumps. We thought that special materials like the ytterbium-doped apatites (Yb:apatites) should exist, and we devised the appropriate means of identifying them.

Apatite is a group of phosphate minerals—there are ten species in all. The Yb:apatites are crystals into which approximately 1% Yb is introduced. We have performed this procedure with four apatite species: fluorapatite,  $\text{Ca}_5(\text{PO}_4)_3\text{F}$ ; strontium-fluorapatite,  $\text{Sr}_5(\text{PO}_4)_3\text{F}$ ; a mixture of these two materials  $\text{Ca}_2\text{Sr}_3(\text{PO}_4)_3\text{F}$ ; and strontium fluorovanadate,  $\text{Sr}_5(\text{VO}_4)_3\text{F}$ . We are the first to grow the last named, and although the other three crystals were known to be growable, we recognized that the Yb dopant gave these materials remarkable laser properties.

The Yb:apatite crystals offer laser properties not previously available from an optical material. (See [Figure 3](#).) Most significantly, they store energy substantially more efficiently (2.5 to 5 times) than standard neodymium-doped laser materials, such as yttrium-aluminum-garnet (Nd:YAG), yttrium-lithium-fluoride (Nd:YLF), and glass (Nd:glass). Efficiency is critical to many diode-pumped solid-state lasers used in applications requiring a specified energy output. For example, if the required solid-state laser energy output is 1 J and lasing and pumping efficiency is 20%, the diode output energy must be 5 J in order to serve as the optical driver. Since the laser material is typically pumped for the same amount of time that the energy will be stored, the required diode power is 5 J per unit storage time. It turns out that Nd:YAG requires 21 kW, but Yb:apatite requires only 4 kW.

The greater storage efficiency reduces the needed investment in the most costly part of the laser system—the laser-diode pump source. This cost generally scales in dollars per watt. At the current cost, about \$20/W, pump

diodes will cost \$420,000 for the Nd:YAG system but only \$80,000 for the Yb:apatite system. Moreover, laser system cost grows in proportion to output energy (in the millions of dollars for a 10-J system). A 10-J pulse of output energy translates into a diode cost of about \$1 million for the Yb:apatite gain medium, less than a third the cost of diode-pumped Nd:glass.

Yb:apatite materials are principally useful for applications requiring a specified energy per pulse from the laser, and especially requiring an energy greater than 1 J. An important example is the printing of circuits by x-ray lithography. Laser x-ray lithography is being developed to support the future productivity and competitiveness of the U.S. electronics industry. Although the methodology has been determined to be viable, the cost of the laser system is a major issue. The laser in current use, a flashlamp-pumped Nd:glass system, is somewhat inefficient and incurs substantial heating, which limits the repetition rate and thus the circuit-production rate. Replacing this laser with a diode-pumped Yb:apatite system will reduce thermal loading by roughly a factor of three and increase overall laser efficiency by a similar factor.

Another application requiring a specified energy per pulse is laser paint stripping (useful for large projects such as bridges, aircraft, and ships). The most common paint-stripping methods are sandblasting and chemical treatment, both of which are expensive and tend to generate substantial pollution. Studies suggest that laser paint stripping is cleaner and more effective—assuming a reliable, efficient, and affordable laser source can be designed and built. A Q-switched diode-pumped Yb:apatite laser may prove useful for this application as well.

Commercial sales of diode-pumped solid-state lasers are modest (approximately \$20 million/yr), although the growth rate is a healthy 15%/yr. However, the overall solid-state laser market is considerably larger (about \$300 million), and diode-pumped solid-state lasers are likely to replace many of today's flashlamp-pumped systems. Diode-pumped solid-state lasers can serve as enabling technologies, enhancing the total benefits of their deployment far beyond their independent value. The potential impact of x-ray lithography on the multibillion-dollar electronics industry is a prime example.

Yb:apatite lasers could replace diode-pumped Nd-lasers in many current applications. They could be used in scientific research systems, serving, for example, as a laser to pump a tunable titanium-doped sapphire or dye laser. They could be used in compact, efficient systems for marking, remote sensing, and medical applications. In material processing, they could perform cutting, welding, and drilling operations.

A particularly exciting possible application for a diode-pumped

Yb:apatite laser could be as a driver for inertial fusion energy. In this application, a certain amount of laser energy (on the order of several megajoules) must arrive at the target to drive it to fusion ignition. Here the storage time has enormous impact on the overall cost of the laser.

*This work was done in cooperation with the Center for Research and Education in Optics and Lasers, University of Central Florida, Orlando, Florida.*

**For further information contact  
Stephen A. Payne (510) 423-0570.**

### High-Precision Low-Noise LVDT Amplifier

The precision manufacturing industry requires increased accuracies in measurement in order to lower production costs by reducing the amount of wasted material; increased accuracies can also yield products with improved performance and wear life. Extremely high accuracies require inspection equipment with very fine sensitivities. One type of sensor for measuring surface irregularities is the

linear variable differential transformer (LVDT). An LVDT is, briefly, a transformer with a primary and two symmetrically offset secondary windings and a movable magnetic core. A stylus-tipped shaft extends from the core and is held in contact with the part to be measured. Displacements of the stylus move the core, changing the magnetic coupling of primary to secondaries and generating a linearly increasing voltage as the core is displaced from its rest (null) position. An air-bearing LVDT provides the ultimate mechanical configuration; it allows stylus force to be adjusted to minimize part deformation and provides nonstick operation for high precision and resolution.

Through an industrial partnership agreement, LLNL and Lion Precision (St. Paul, Minnesota) jointly developed a precision amplifier for use with the LVDT. This high-gain, low-noise, air-bearing amplifier offers 30 to 40 times better resolution than other high-precision measurement devices using a similar sensor. Contact displacement measurement resolution is near the atomic level: coupled with an air-bearing LVDT, the amplifier's sensitivity and unique circuitry provide resolution to two atomic diameters, or 0.6 nm. Over its range of travel, it rivals the resolution of high-precision displacement-measuring laser interferometers.

The amplifier also provides very high gain, or increase, in signal power—100 to 1000 times that of competitors—while requiring 5 to 10 times less excitation of the sensor than competitive products. Minimizing sensor excitation reduces LVDT heating, decreasing thermal distortion of the part being measured, thus providing higher precision and repeatability. The amplifier provides a fixed-frequency, highly stable primary excitation signal. The secondary signal is amplitude modulated by the core position

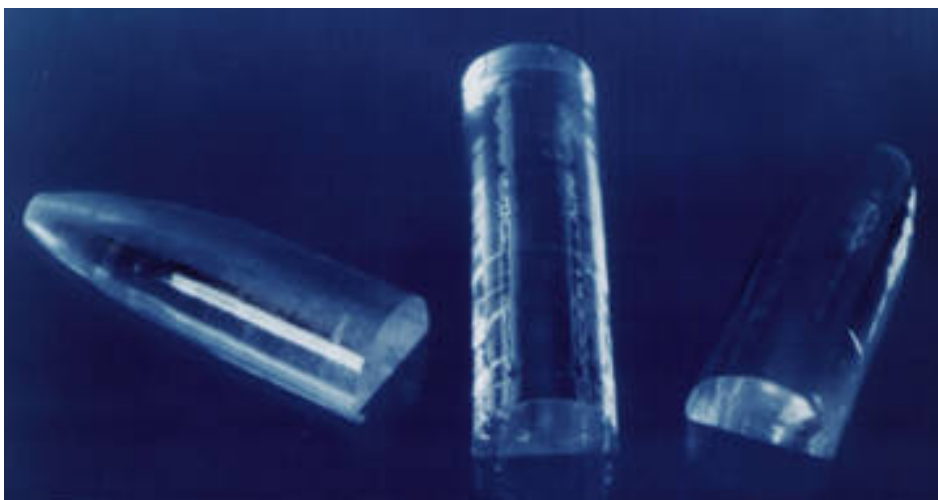


**Figure 3.** Several crystals of Yb:apatite, showing that they can be grown in large sizes (7.5–9 × 2 cm) and with high optical quality.

(dictated by the displacement of the stylus). A phase-sensitive detector demodulates position information returned from the LVDT secondaries. Resolution is almost infinite and depends on the signal-to-noise ratio of the signal-conditioning electronics. By providing constant current excitation of the LVDT, our amplifier provides the same level of coupling to the secondaries even if coil resistance changes because of temperature changes.

The LVDT signal has one desired component (the displacement signal) and one undesired. The amplifier has a circuit to handle each: one circuit maximizes the desired signal amplitude; the other cancels the undesired signal before it can saturate any predetector amplifiers. Predetector gain is maximized and postdetector gain minimized. Cancellation of the undesired signal is one of the reasons this amplifier easily outperforms the resolution of the next-best amplifiers. Resolution better than 2.5 nm is possible with a 100-Hz bandwidth, and 0.6 nm with a 2.5-Hz bandwidth.

Machine tool builders, metrologists, and quality inspection departments can now measure surface irregularities as tiny as 1/120,000 the width of a human hair. Indeed, principal applications include machine tool metrology, coordinate measuring machines, diamond-turning machines, roundness gauges, and precision manufacturing. Parts made at LLNL by machines such as the Large Optics Diamond Turning Machine—the world's most accurate diamond turning machine—typically require that the part be measured to better than 2.5 nm and part surface finishes to better than 12.5 nm. This amplifier can immediately improve measurement resolution of inspection machines.

The amplifier can replace signal-conditioning electronics for any sensors

using LVDT technology, such as load cells for measuring force or torque, pressure measurement sensors, accelerometers, and inclinometers. Future applications include metallurgical research and use by the semiconductor industry to measure the thickness of thin-film deposits on microelectronic components.

This amplifier advances contact displacement measurement to the same accuracy and resolution commercially available until now only from noncontact displacement measuring systems, such as capacitance gauges and interferometers. For many tasks, such as measuring small objects that are nonconducting or are not completely free of oil or coolant, capacitance technology is inappropriate. Although capacitance gauges measure contour figure with

high resolution, they provide poor spatial resolution and therefore cannot measure part surface finish. Laser interferometers require a reflective mirror surface to return the beam, so direct part measurement is normally not possible. Moreover, interferometer systems are more complex, larger, and more costly to use than the LVDT amplifier. (The amplifier can also be configured for noncontact displacement measurement. Resolution is at the atomic diameter level.) Thus, this amplifier breaks new ground in defining the state of the art in contact displacement measurement.

*This work was performed under a cooperative research and development agreement (CRADA) with Lion Precision, St. Paul, Minnesota.*

**For further information contact David Hopkins (510) 423-6134.**



**Figure 4.** The amplifier (left), shown next to a part under inspection; the LVDT probe extends from the tool bar of the Large Optics Diamond Turning Machine. The part under inspection is the Keck II secondary mirror for the Keck Observatory in Hawaii.

## Silicon Microbench Technology

Most fiber optic communication is now done at rates below 1 gigabit (1 billion bits) per second (Gb/s). The dimensions of the multimode fibers used at these rates allow component-alignment tolerances of several tens of micrometers. New communications standards are designed for operation well above 1 Gb/s. Such high speeds require that much finer single-mode optical fiber be used. This fiber must be aligned to single-mode optoelectronic components at submicrometer tolerances. Achieving these tight

tolerances using current cumbersome manual alignment and attachment (pigtailling) techniques takes extraordinarily long times. These times drive up the costs of packaging, which can account for as much as 95% of the cost of optoelectronic devices. The most time-consuming and, therefore, most expensive part of the packaging is the alignment and attachment of the fiber. Today, each single-mode packaged device typically costs several thousand dollars.

We are developing automated alignment and attachment techniques to reduce the cost of packaged opto-

electronic devices. Our mounts provide the stability and localized heating to achieve the tight tolerances while simplifying assembly and allowing relatively inexpensive mass production. Volume production is the key to reducing costs 10 to 20 times, to less than \$10 a device for the packaging cost.

The key to mass production is to reduce the time per "pigtail"—the packaging operation of joining an optical fiber to an optoelectronic device, such as a laser. We are building a fiber pigtailling machine that will automatically align a fiber to a laser diode or to a lithium niobate modulator with submicrometer accuracy in less than 5 minutes. (At volumes of several thousand pigtaills per year, the cost per manual pigtail approaches \$100, whereas at volumes of several tens of thousands per year, the cost per automated pigtail is less than \$10.) We designed and built silicon substrates with geometries that are compatible with the automated processes and have the stability required to maintain the submicrometer alignment tolerances necessary for single-mode operation. These substrates are the key part of an automatic alignment package.

We have designed our mounts with discrete areas for optoelectronic device attachment and areas for fiber attachment. For example, the 13- × 6-mm mount shown in Figure 5 is for packaging a 1550-nm distributed feedback laser. On the left half, gold pads provide a ground plane for the laser and stress relief for the wire bonds. To attach the fiber on the right half of the mount, two polysilicon heating elements are connected to gold bonding pads for electrical contact. In the center of each heater, a 1- × 0.5-mm gold solder attachment base (on a layer of silicon dioxide for electrical isolation from the polysilicon heater) is large enough for a 125- $\mu$ m-diameter

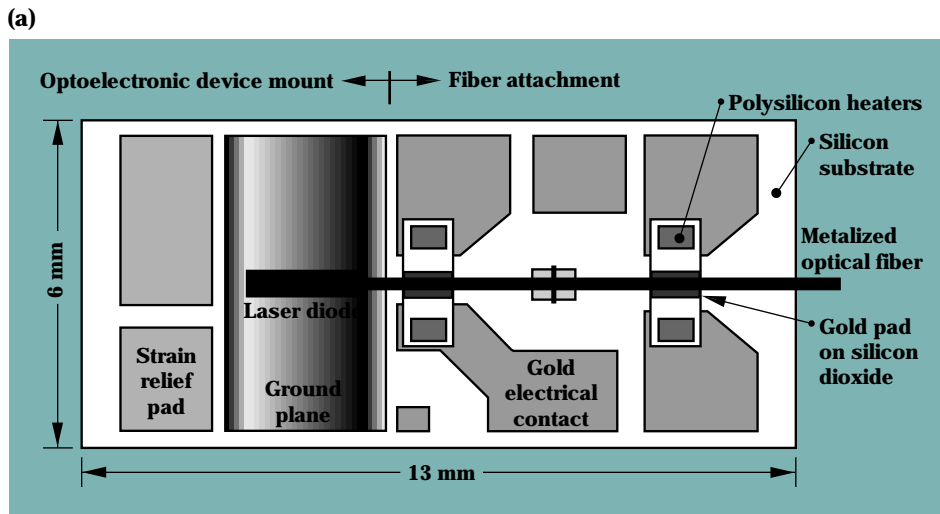
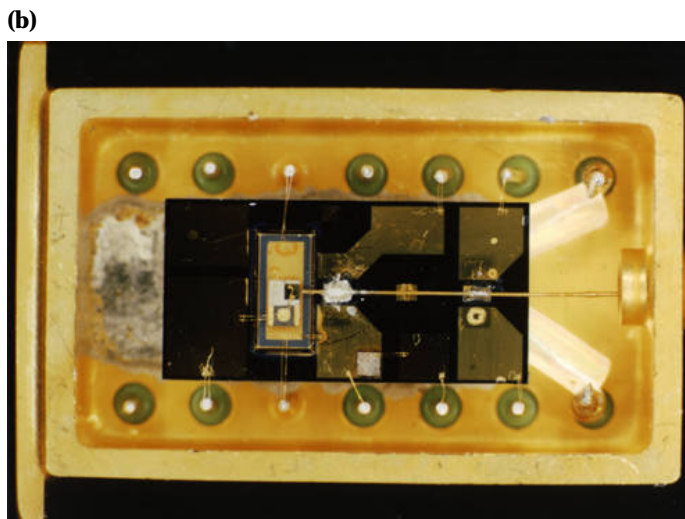


**Figure 5.** (a) Sketch of silicon mounts showing the location of the components and heaters. (b) Photomicrograph of a silicon mount inside a standard gold-plated metal package with a laser diode. A metalized optical fiber is mounted and aligned to the diode. The silicon mount is 6 × 13 millimeters.



fiber to be soldered to it. We use either 100- $\mu\text{m}$ -diameter solder balls or solder paste to attach the metalized fiber.

A simple power supply and a timed switch allow us to control accurately the magnitude and time of the applied current, giving our prototype very reproducible performance. We use active feedback to align the fiber to submicrometer accuracies. While the fiber is held in the position that maximizes the optical coupling, current is passed through the heater to reflow the solder, which wicks around the metalized fiber without disturbing the automatic submicrometer optical alignment. Conventional techniques for melting solder heat the entire substrate, creating considerable difficulty with drift of the alignment after the solder has cooled and requiring such corrective measures as preshifting the fiber so that after cooling the thermal shifts will tend to bring the fiber into alignment. By providing only the small amount of heat needed to melt the solder locally, we avoid these thermal shifts and greatly simplify the alignment process. We observe no decrease in the light coupled from a 800-nm laser diode into the single-mode fiber after the solder has cooled.

Silicon mounts offer the additional benefit of allowing us to use standard, low-cost silicon etching techniques to bring the optical axis of different components in approximately the same line vertically (see **Figure 6**), minimizing the solder thickness and therefore thermal drifts and long-term creep that are problems with other packages that use thick solder or metal "shims" to bring the optical axis in alignment.

The potential market is enormous. As fiber communication products become more prevalent, one can envision these packages used at either end of every fiber for transmitters and receivers of high-speed optical signals. At sufficiently low production costs,

the market is potentially many millions to billions of devices in a multitude of applications, ranging from single-mode fiber-optic communication products and laser-diode transmitters, to the assembly of hybrid optoelectronic multichip modules and fiber arrays, semiconductor optical amplifiers, fiber-optic gyroscopes, optical interconnects for computer backplanes, asynchronous transfer mode (ATM) switches, all optical switches, and optical modulator arrays.

Our mount geometries with on-board heaters allow rapid attachment of not only the fiber but other components as well. Using solders with different melting temperatures and attaching components farthest from heaters first allow sequential mounting of several components on the same silicon mount without melting solder and disturbing the alignment of previously attached components. Since many components do not require submicrometer alignment, we envision that an automated system could place and solder them onto the mounts in only a few seconds.

On-board heaters can be used in applications other than packaging laser diodes. For example, we are designing a longer mount with heaters at each end to pigtail both ends of a semiconductor optical amplifier. We are also investigating geometries compatible with high-speed applications in which on-board transmission lines will be needed to provide sufficient electrical bandwidth for the very high-speed optoelectronic devices.

*For further information contact Michael Pocha (510) 422-8664.*

## Chromosome-Specific DNA Probes for the Mouse

We have developed DNA reagents, or probes, that color or "paint" chromosomes of the laboratory mouse to make them instantly identifiable. Chromosomes are made up of complex folded strands of DNA that contain the genetic information (genes) inside each cell of an organism. Our DNA

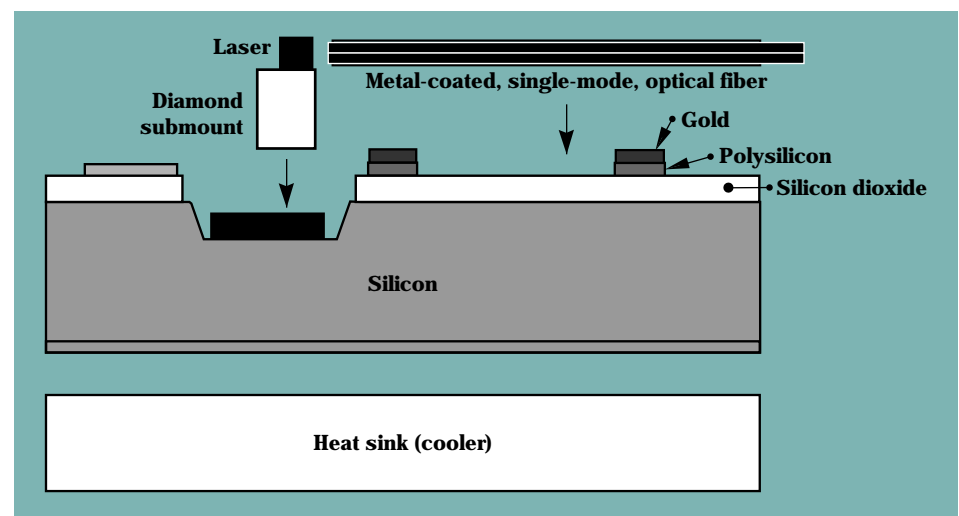


**Figure 6.** Cross section of a mount showing precision-etched well for laser diode to help vertically align the optical axis.

probes can clearly and distinctly identify one or more of the 20 pairs of chromosomes that are normally found in mouse cells. **Figure 7** shows painted mouse chromosomes and a similar cell stained by the old method of chemical staining or banding. Painting clearly identifies eight of the 40 chromosomes, permitting several chromosomes from each cell to be rapidly and distinctly identified, even by a novice investigator. Identifying them by the old method is difficult, even for someone highly trained, because of the similarity in size of chromosomes from the mouse.

Each probe is a mixture of thousands of different DNA sequences, each present in thousands of copies. The probes are mixed in solution and placed on a microscope slide over the area to be stained so that the probes anneal, or stick, to the target

chromosomes. For painting to be specific to a single chromosome type, all the DNA in a probe must be derived from only that designated chromosome.

Painting probes are commonly used to detect chromosome rearrangements, and this method is more than 60 times faster than the standard chemical staining or banding method. Painted chromosomes are so simple to analyze that we have taught this method to new people in 2 hours. With chemical staining, highly skilled personnel must be employed. Thus, when cost and speed are both considered, painting is up to 200 times more efficient than banding.

The DNA probes we developed for the mouse have numerous applications, many of which relate to cancer and birth defects.

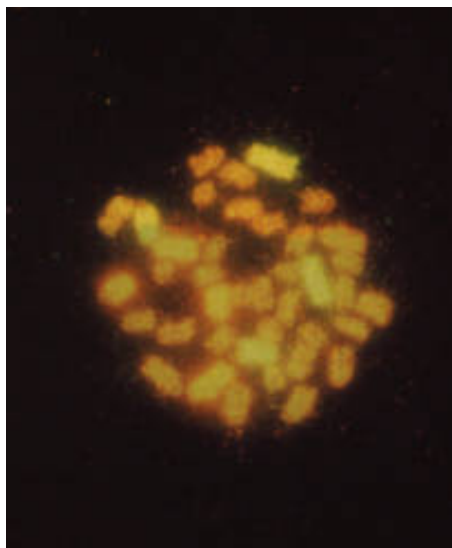
**Toxicology.** We developed our probes to apply chromosome painting

to toxicology. We are using them to evaluate two cancer-causing chemicals found in food and will soon evaluate two more cancer-causing chemicals found in drinking water. We are also painting cells from mice exposed to ionizing radiation, which also causes cancer. For each study, we screen cells like those in **Figure 7** for rearrangements between painted and unpainted chromosomes. Rearranged chromosomes appear bicolored, for example, red at one end and yellow at the other.

These probes make it easy to detect a class of chromosome rearrangements called translocations. Unlike other rearrangements, translocations are stable through cell division; thus, their frequency does not diminish with time, they accumulate for as long as exposure to chemicals or radiation continues, and they persist after exposure terminates. Translocations do not always change the length of a chromosome and thus are difficult to detect. As a result, before the advent of painting, toxicologists performing chromosome analyses generally did not consider translocations. Virtually all humans experience long-term adverse environmental exposure—DNA-damaging chemicals are found in cooked food, diesel exhaust, and some drinking water, to name just a few sources. Natural background radiation is also ubiquitous; one example is radon. Until now, the understanding of how chronic exposure to these and other agents affects human health has been limited. These mouse-painting probes permit the development of an animal model to test the effects of these exposures.

**Birth Defects.** DNA probes for the mouse will also aid studies of factors that cause sperm to have the wrong number of chromosomes, which leads to birth defects.

(a)



(b)

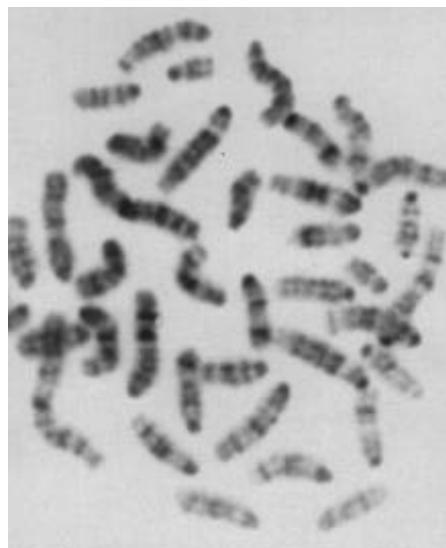


**Figure 7.** (a) Mouse chromosomes, from a single cell, painted with DNA probes for chromosomes 2 and 8 (red) and chromosomes 1 and 3 (yellow). These chromosomes are distinguished from the others by their color. (b) Mouse chromosomes from a single cell stained by the chemical staining or banding method. The black and white bands are used to distinguish one chromosome from another.

**Tumor Research.** Tumor cells typically have alterations in chromosome number and size, and these abnormalities are notoriously difficult to evaluate with standard banding methods. Chromosome painting can be used to solve this important problem.

**Mouse Genome Project.** The goals of the mouse genome project include identifying, locating, and characterizing each of the 50,000 to 100,000 genes in the mouse. More is known about the genetics of the mouse than any mammal except the human, and discoveries in the mouse frequently lead to an improved understanding of human biology. Genes found in one species frequently have a counterpart in the other, and the identification of a gene in the mouse greatly simplifies the process of locating the corresponding human gene. Our probes have been made available to one of the leading laboratories working on this project.

**Genetic Research.** Gene mapping, or locating a gene on a chromosome, is frequently an important step in the process of obtaining and cloning a new gene. We have used our probes to map a gene onto a mouse chromosome by performing dual-color hybridizations. We labeled the DNA for the gene in yellow and DNA for the chromosome painting probe in red. The chromosome bearing the gene was identified by a yellow hybridization signal on an otherwise red chromosome. The simplicity of this method suggests that it will be used more widely by ourselves and others in the future.

**Pharmaceutical Research.** The most significant potential application of these mouse chromosome painting probes is their use by pharmaceutical companies, which must assure the Food and Drug Administration that

new drugs are safe to market. The battery of tests include genetic assays designed to determine whether the compound breaks chromosomes. If it does, it is very unlikely to be approved for clinical use, because chromosome breakage is associated with cancer and birth defects.

In many chromosome breakage assays, mice are given a single exposure to a drug at a much higher dose than people would normally be given, and their chromosomes are examined a day or so later. This exposure method is unrealistic because most drugs are taken by people at low doses over a period of days, weeks, or even years. Indeed, toxicology assays that involve lower, more realistic, doses are also performed on mice. However, testing for chromosome damage as part of these protocols is difficult because a good method of quantifying stable translocations from a large number of cells has been lacking. The tremendous sensitivity of our mouse probes has enabled us to quantify stable genetic damage following chronic exposure at lower doses. Mouse chromosome painting for translocation analysis could be coupled with existing drug testing protocols to provide improved estimates of chromosome damage under realistic exposure scenarios.

The development of chromosome-specific composite DNA probes for the mouse promise a significant impact on human health with long-term benefits. The primary benefits include:

- An improved understanding of how chronic exposure to chemicals and radiation affects human health.
- The genetic testing of potential pharmaceutical drugs at realistic exposure levels.
- An improved ability to use the mouse for mapping and cloning important new genes.

- An improved understanding of the chromosomal changes involved in tumor formation.

*For further information contact James D. Tucker (510) 423-8154.*

## Summary

R&D 100 awards are given for processes and products that the panel of judges considers to promise significant contributions to the quality of life in the United States and throughout the world. Past award winners have indeed improved the ways people do such things as communicate, transact business, spend their leisure time, maintain health, and fight disease. We at Lawrence Livermore National Laboratory are gratified that in the 30-odd years that the award has been given, we have won 50, six of them in the last year alone. These awards signify that the Lab's work has been valuable not only for maintaining national security in the past, when defense research was necessarily the largest single component, but for advancing it now, when the mandates of economic competitiveness—speed, efficiency, and quality—give urgency to our work.

# Legacy of the X-Ray Laser Program



*The X-Ray Laser Program, which was stimulated by a vision of a laser system that could provide strategic defense against Soviet missiles, has left a legacy of new technologies for industrial and medical use.*

**I**NTEREST in producing shorter wavelength lasers that reached into the x-ray region began soon after the first ruby laser was operated in 1960. With the advent of the large lasers for inertial confinement fusion in the early 1970s, several groups, including those at Lawrence Livermore National Laboratory, proposed studies of nuclear and nonnuclear pumped x-ray lasers.

On March 23, 1983, President Reagan challenged the scientific community to find a defense against nuclear-tipped ballistic missiles. As the technical committees formed in response to this challenge focused largely on antiballistic missile systems, an alternative approach proposed

accelerating an LLNL research program that was working on a nuclear-pumped x-ray laser system. If successful, such a system might offer a shield for the United States in the event of nuclear war. Thus began the funding of the x-ray laser effort and numerous other research activities (such as the efforts in free-electron and chemical lasers and Brilliant Pebbles, a nonnuclear antiballistic missile concept) under the Strategic Defense Initiative (SDI).

Since 1983, the world has changed dramatically. The Berlin Wall has fallen, Germany has been reunited, and the Soviet Union has collapsed. Because of these changes and the various technical difficulties involved

in developing the x-ray laser into an antiballistic missile system, the X-Ray Laser Program has been eliminated. However, many of its technical and physics achievements live on in areas unrelated to strategic defense.

We are finding that much of the x-ray laser technology originally developed for strategic defense can be used to advance research in biotechnology, materials science, and materials analysis.<sup>1</sup> This rich legacy includes a better understanding of x-ray laser physics; an array of sophisticated computational tools for modeling plasma physics; a laboratory x-ray laser for biological imaging; the development of such advanced materials as aerogel and SEAgel;

a unique, world-class research facility, called the electron-beam ion trap (EBIT), for performing atomic physics experiments; new measurement techniques for characterizing materials; and a superior mammographic technique for early detection of breast cancer.

### Advancing the Laboratory's Research Goals

To achieve the goals of SDI as it was first envisioned, scientists needed to overcome many of the obstacles they had encountered in trying to better understand the atomic physics of highly charged ions. They also needed more exact measurement systems for nuclear tests and more sophisticated computer programs to process and model the data. Many of our efforts not only improved the quality of our research for SDI but were also transferred to research in other areas.

### Diagnostics

In the 1970s, most measurement systems for nuclear tests relied on coaxial cables connected to single x-ray diodes. As electronics technologies were improved, coaxial cables were replaced by fiber optics, streak cameras, multiplexing, and other new technologies. With the advent of the x-ray laser effort, scientists suddenly needed vast quantities of high resolution data that could not be gathered by using conventional techniques. This need for more detailed data pushed the immense growth in the development of advanced electro-optic devices used in nuclear tests.

### Transmission Crystal Spectrometer

A good example of the tremendous progress in measurement systems technologies is the transmission crystal spectrometer (TRACS).

Before the development of this spectrometer, hard x rays were measured in the nuclear environment using absorption-edge filters and fluorescers to define bandpass regions of the x-ray spectrum. This diagnostic approach could accommodate very few data channels, and therefore, the amount and type of data that could be gathered were severely restricted. For example, a standard instrument like the SPECTEX had 10 spectral-energy channels. The TRACS solved the crystal spectroscopy problem by providing a way to measure short wavelength x rays (i.e., hard x rays) by using a crystal with the planes perpendicular to the crystal surface, as shown in **Figure 1**, and then measuring the transmission spectroscopy of the x rays. The x rays still have small Bragg angles with respect to the Bragg planes, but now they strike the crystal at near-normal incidence. Using the TRACS one can now have 1000 channels of time-resolved data covering the same

spectral range as the SPECTEX, an increase of two orders of magnitude (100 times) in resolution.

### High-Precision Spatially Resolved X-Ray Spectrometer

Measuring the electron temperature of a plasma is very important to our understanding of the dynamics of nuclear-driven plasmas. To gather this type of information, a high-precision spatially resolved x-ray spectrometer was developed that measures the free-bound continuum emission from radiative recombination. In one particular experiment, four samples were imaged simultaneously with subnanosecond time resolution. This required very stringent pointing tolerances that were not previously possible. A 20- $\mu$ rad pointing accuracy was achieved, which was 5 times better than the 100- $\mu$ rad resolving power of the spectrometer. The electron temperatures of both the K- and L-shell nuclear-driven plasmas were determined to an accuracy of better than 10%.

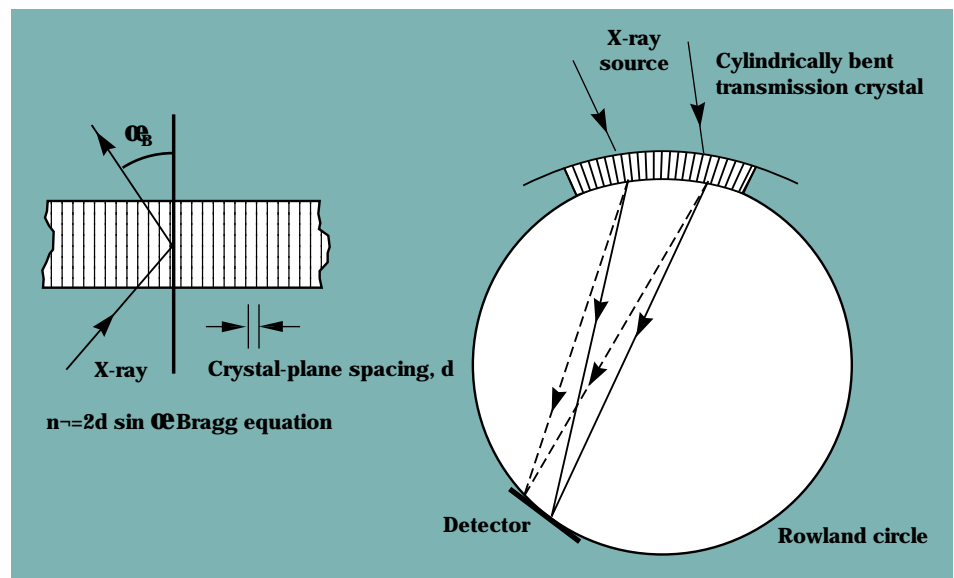


**Figure 1.** Transmission crystal spectrometer (TRACS) for measuring hard x rays underground. The TRACS uses a crystal with the planes perpendicular to the crystal surface, and measures the transmission spectroscopy of the x rays.

## Fast X-Ray Detectors

A new generation of fast x-ray detectors was developed to meet the challenges of diagnosing plasmas in a nuclear environment. The new detectors are based on microchannel plate-intensified detectors developed for diagnosing laboratory x-ray lasers. These detectors have a 400-ps time resolution and convert the x-ray signal into an optical signal 1000 times brighter than the x-ray signal. This is a million-fold conversion efficiency enhancement when compared with the passive phosphors and scintillators used previously. **Figure 2** shows a schematic of the detector with the photocathode that converts x rays to photoelectrons, the microchannel plate (MCP) that amplifies the photoelectrons, the electrostatic focusing electrode that compresses the electron current in one dimension, the fast phosphor that converts the electron's kinetic energy to light, and the fiber-optic face plate that transmits the light out of the vacuum system.

## A Laboratory X-Ray Laser

Research on the laboratory x-ray laser began as part of the effort to

improve our understanding of x-ray laser physics and to develop laser physics computation codes. To design this laser, we needed very complex atomic models that could be used for solving plasma kinetics. As a result, we developed several computer codes, such as YODA, ADAM, and XRASER. In the first experiments, we used the Novette laser, a prototype for the Nova laser, to study x-ray laser physics. In 1984, we demonstrated the first laboratory x-ray laser.

As a result of these tests, the Defense Sciences Department funded a second target chamber on the Nova laser that would allow two beams for x-ray laser experiments. This two-beam facility has been in use for 10 years and has demonstrated many new x-ray lasers, with wavelengths ranging from 32.6 nm in neon-like titanium to 3.5 nm in nickel-like gold.

## X-Ray Imaging

One potential use of a laboratory x-ray laser is in imaging. X-ray lasers are being coupled with x-ray microscopes to image biological samples. Using x-ray lasers as a light source, we may be able to use x-ray

microscopes to image live hydrated organisms to better understand the structure of a living organism. Our goal is to use this technology to create three-dimensional (3-D) holograms of living organisms. As the first step toward making these images, we have constructed an x-ray microscope that uses a 4.483-nm nickel-like tantalum x-ray laser as the light source. The wavelength of this laser is ideal for biological imaging because it provides good contrast between the carbon in the living organism and the water in which the organism lives. A spherical multilayer mirror condenses the light onto the target, and a zone plate lens projects the image onto the microchannel-plate detector (**Figure 3**).

We are using this technology to study how DNA is organized inside a sperm cell. **Figure 3b** shows an image of rat sperm that was taken with our x-ray microscope; this particular microscope is powerful enough to detect features as small as 50 nm.

To improve the coherence and power of x-ray lasers, we demonstrated multipass amplification at 20.6 nm in a neon-like selenium laser. We placed a flat multilayer mirror made of

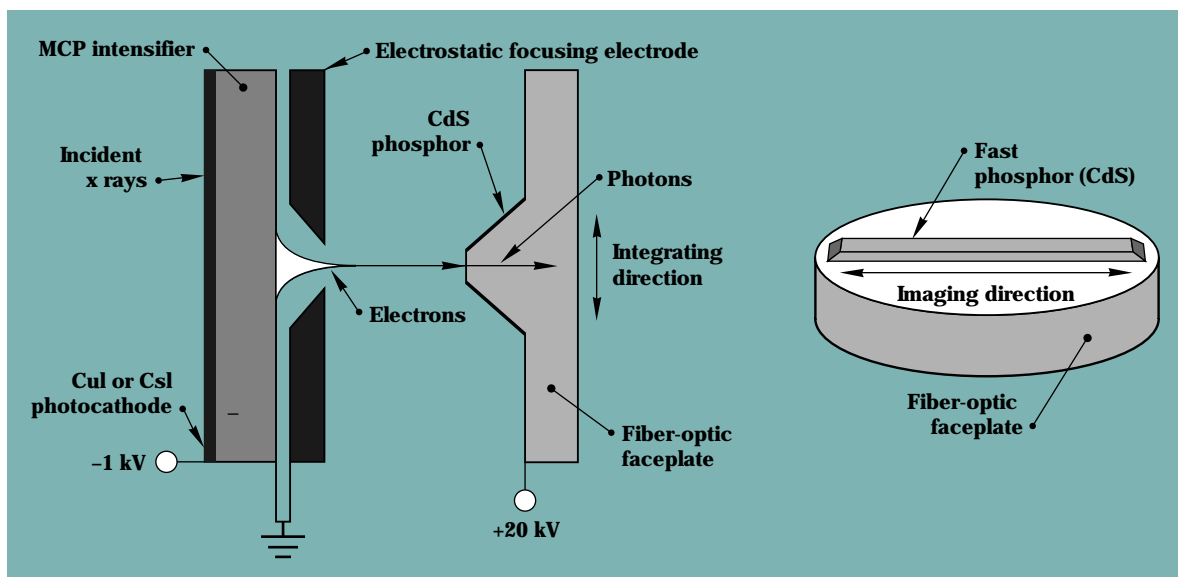


**Figure 2.** Time-resolving intensified detectors for low-level x-ray detection. The photocathode converts x rays to photoelectrons and the microchannel plate (MCP) intensifier amplifies the photoelectrons. The electrostatic focusing electrode compresses the electron current in one dimension, and the CdS phosphor converts the electron's kinetic energy to light. Finally, the fiber-optic faceplate transmits the light out of the vacuum system.

30 molybdenum–silicon pairs 2.75 cm from the end of the laser medium. Data collected at the right end of the laser (Figure 4) showed both the amplified spontaneous emission (ASE) pulse from x rays that originated at the left end of the laser (these x rays were amplified as they propagated down the length of the laser) and a second pulse created by x rays starting at the right end. This second pulse was observed after it propagated down the laser, was reflected by the mirror, and then was reamplified during its second pass through the gain medium (Figure 4a). The double-pass amplified signal was seven times more intense (Figure 4b) than the single-pass ASE. This experiment demonstrated the first step toward making an x-ray laser cavity, which offers the potential for producing the highly coherent output required to do holography.

Multilayer mirrors have also been important in developing new diagnostics in the soft-x-ray regime, where crystal spacings are too small to allow measurements to be made. The multilayer mirrors are essentially crystals with layer spacings that are matched to the long wavelengths

being diagnosed. A variation of the multilayer technology is the Fresnel zone plate, which is essentially a multilayer mirror rotated 90 degrees.

A tabletop x-ray microscope that achieves 10- $\mu\text{m}$  resolution has been built using 8-keV Fresnel zone plates. This microscope creates images of a sample by scanning it with a focused x-ray spot that is produced by a phase-modulating zone plate and a copper K- $\alpha$  source. The picture of the ant shown in Figure 5 is an example of an image made using this microscope.

### New Materials

Another outgrowth of the X-Ray Laser Program was the research and development done in very low-density foams, such as silica aerogels, organic aerogels, and safe-emulsion agar gel (SEAgel). Aerogels are solid foams so low in density that they are mostly empty space. They are open-cell structures, like a sponge, with tiny pores (< 50 nm in diameter). Because both the particle and pore sizes are much smaller than the wavelengths in the visible spectrum (350 to 800 nm), aerogels are transparent to visible light.

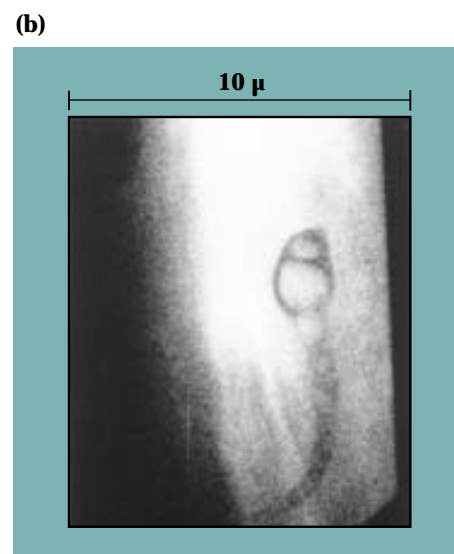
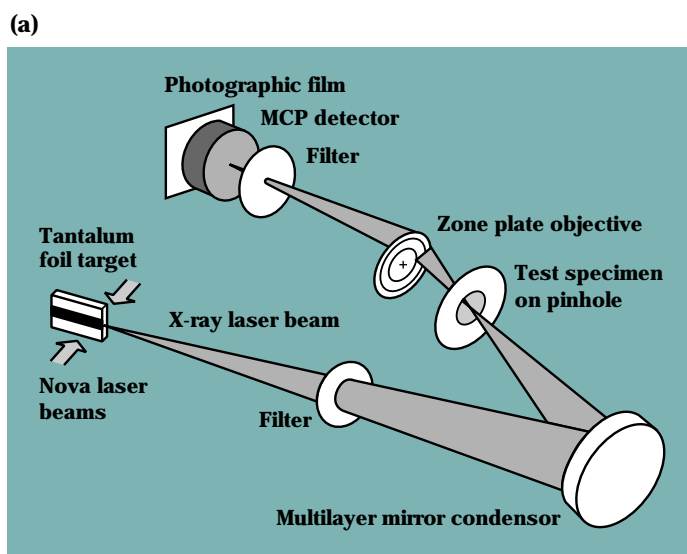
Silica aerogels—highly porous forms of silica or silicon dioxide ( $\text{SiO}_2$ )—were first prepared in the 1930s at Stanford University, but they were not put to practical use until the 1970s, when they were used in nuclear-particle detectors. In the 1980s, Laboratory scientists working in the X-Ray Laser Program extended aerogel technology by creating superlight silica aerogels (with densities of 1 mg/cm<sup>3</sup>) and by producing organic aerogels.

Aerogels have outstanding thermal insulating and acoustic properties. Because they transmit heat at only one-hundredth the rate of full-density glass, a 1-cm-thick aerogel panel insulates as effectively as a 4-cm-thick batt of fiberglass. They are natural candidates for insulation in window glass, refrigerators, and other appliances. Figure 6 vividly illustrates the insulation value of aerogel. In this photograph, a person is holding a piece of aerogel foam while he heats it with a blowtorch. The aerogel foam effectively protects his hand from the flame of the torch.

Aerogels also can be used in space to collect fast-moving particles, such as micrometeoroids (cosmic dust).

### Figure 3.

(a) Diagram of the x-ray microscope. The light source is a nickel-like tantalum x-ray laser. The x-ray laser beam is condensed using a spherical multilayer mirror, and a zone plate projects the image onto the microchannel-plate detector. (b) Image of rat sperm captured using the x-ray microscope. This image shows 50-nm features.



Organic aerogels are likely to be used as gas filters in chemical processing, as catalyst beds for the petroleum industry, and as thermal insulators for cryogenic applications.

SEAgel, a very low-density, organic-based foam (Figure 7), is a natural material made from agar—a component of red algae that is used to thicken ice cream and other foods. SEAgel is made by dissolving agar in water and adding an organic solvent and emulsifier that disperse the agar evenly throughout the liquid. Then the mixture is freeze-dried to extract the water and solvents. SEAgel can be made with densities from 1 to 300 mg/cm<sup>3</sup> and with cell sizes from 2 to 3 μm.

Laboratory scientists are using SEAgel as targets for x-ray laser experiments on Nova because it can be doped with other materials, such as selenium. If we can fabricate an x-ray laser target with a density that is less than the critical density of laser light ( $4 \times 10^{21}$  electrons/cm<sup>3</sup> for 0.53-μm light), we can eliminate the violent hydrodynamics that take place when a solid-density target explodes before it reaches the density required for lasing. Using SEAgel will help us achieve a more uniform plasma, which will improve the quality of the x-ray laser beam.

Because SEAgel is safe enough to eat, it could be used as food packaging or as encapsulating material for timed-release medication. SEAgel could also be used instead of balsa wood to insulate supertankers and to provide sound damping in high-speed trains.

### The Electron-Beam Ion Trap

The X-Ray Laser Program required a new level of understanding and new measurements of the atomic physics of highly charged ions. The electron-beam ion trap (EBIT) was developed and built at LLNL to study

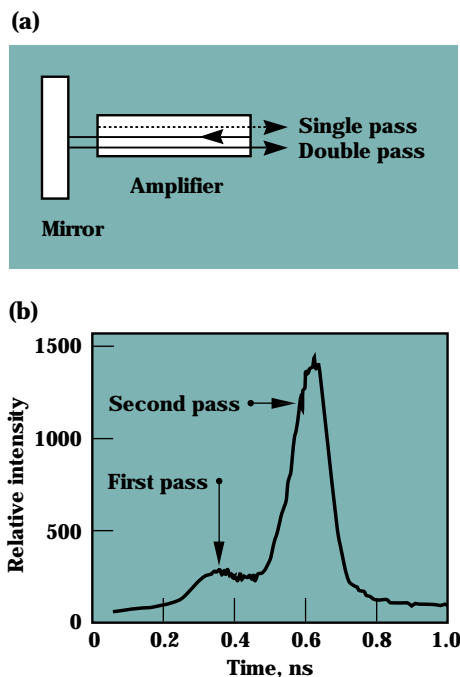


**Figure 4.** (a) Multipass amplification process and (b) measurements from multipass amplification of the x-ray laser. X rays in the first pulse originated at the left end of the laser and were amplified as they propagated down the length of the laser. X rays in the second pulse originated at the right end of the laser, were reflected by the mirror, and then were reamplified during their second pass. As the measurements show, multipass amplification increased the coherence and power of the laser—the double-pass amplified signal was seven times more intense than a single-pass signal.

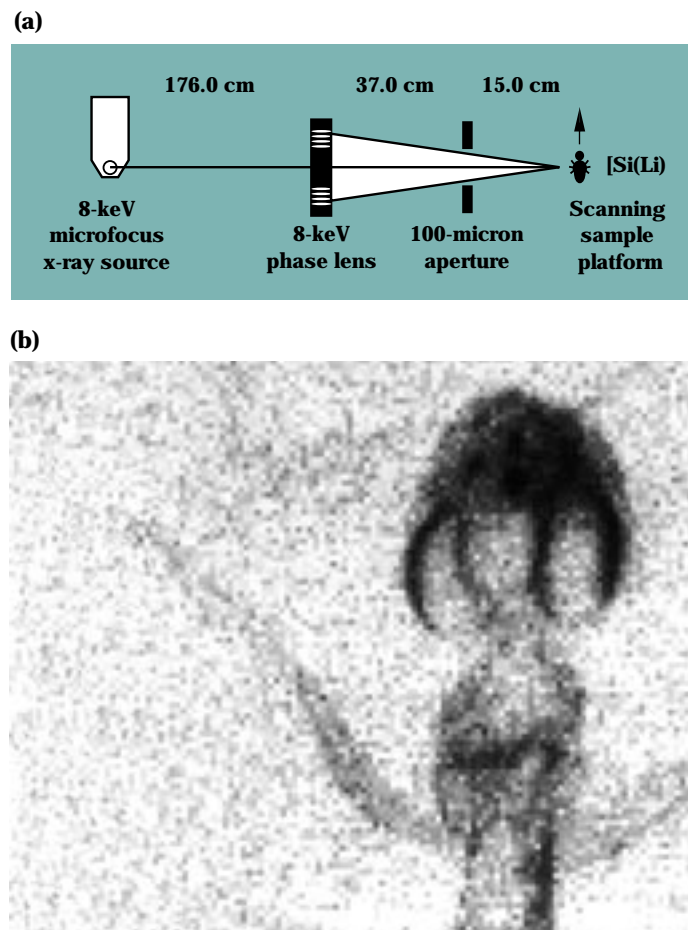
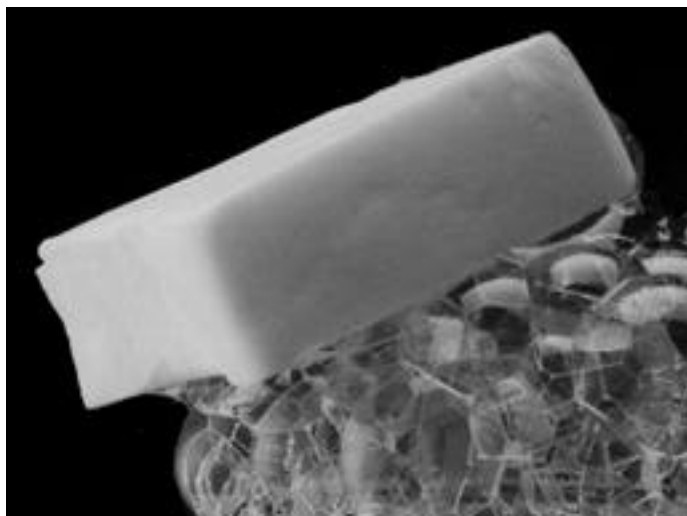


**Figure 5.** (a) Schematic of the 8-keV scanning x-ray microscope geometry and (b) image of an ant made with this microscope. The tabletop x-ray microscope creates images by scanning a sample with a focused x-ray spot that is produced using a phase-modulating zone plate and a copper K-α source. The image of the ant shows features as small as 50 μm; each pixel = 15 μm.

**Figure 6.** Tom Tillotson, a chemist at LLNL, applies a propane torch to the top of a 2.5-cm-thick silica aerogel brick. His hand remains totally unaffected by the heat.



**Figure 7.** A piece of SEAgel floating on soap bubbles in a beaker. This very-low-density organic-based foam, made from the food-thickening agent agar, is safe enough to eat and could be used as food packaging or encapsulating material for timed-release medication.



the behavior of these ions (Figure 8). Currently, EBIT can produce highly charged ions up to neon-like uranium, in which 82 of uranium's 92 electrons are removed (leaving 10 electrons, like neon).

In EBIT, the ions are electrostatically trapped for minutes to hours in a narrow cylindrical volume that is defined by biased electrodes in the axial (longitudinal) direction and by a high-current-density electron beam in the radial direction. The energy of the electron beam can be varied reliably from 2 to 25 keV. This is sufficient to strip all electrons from elements up to molybdenum (creating a +42 charge state) and to make any naturally occurring element neon-like (10 electrons remaining, up to a +82 charge state).

EBIT allows us to measure directly processes that are crucial to understanding high-temperature plasmas. These processes include electron-impact ionization, excitation, and recombination. Before EBIT, only a few measurements of ionization cross sections were available for charge states of 50 or less, and direct measurements of electron impact excitation, dielectronic recombination, and radiative recombination cross sections were possible only for charge states of 6 or less.

The physics of these highly charged ions is of interest as we strive to obtain a fundamental understanding of matter. With EBIT, we can obtain experimental data that allows us to confirm or disprove theoretical predictions. Specifically, we use high-resolution, well-calibrated spectrometers to measure the x rays that result from the inelastic collisions of the highly charged ions with the free electrons in the EBIT electron beam.

We have used EBIT to measure the dielectronic recombination cross section for neon-like xenon (xenon stripped

of all but 10 of its 54 electrons, in a +44 charge state). The EBIT measurements are in good agreement with the theoretical calculations for this cross section. This is an important finding since dielectronic recombination is an important process in theoretical models of the ionization balance in plasmas of neon-like and nickel-like lasers. Before EBIT, measurement of cross sections was possible only for ions with a few electrons removed; now highly ionized materials, such as these plasmas, can be studied. The agreement between calculation and measurement gives us confidence that our theories about the behavior of plasmas and highly charged ions—and essentially our basic understanding of matter—are correct.

With the recent construction of the new super-EBIT, which has beam energies up to 200 keV, we can now strip all the electrons from any ion, including uranium, and therefore study any charge state of any ion. This ability allows the study of even more fundamental tests of quantum electrodynamic (QED) theory.

### Materials Analysis

When we build experiments like those to be included with a nuclear test, we must follow strict manufacturing tolerances. To meet these tolerances, we have developed several characterization techniques that can handle thousands of new parts a year, and many of them, our radiographic methods in particular, have applications in the biomedical industry. For example, we have used our diagnostic technique for finding tiny flaws in SDI components to detect flaws in samples of material used for artificial heart valves. This application is extremely important, considering that 1.5 million people have artificial heart valves and that even the slightest flaw in these valves can be fatal. In these diagnostic experiments, the sample material is

placed in a vacuum chamber and bombarded with a 10-MeV proton beam. The sample is then analyzed by a detector that measures the beam's energy. The thickness of the material is determined by the amount of energy loss in the beam. In recent

experiments, we were able to detect a minute scuff in the core of a sample of carbon-based heart valve material.

Three-dimensional x-ray computer tomography (CT), which was originally developed to inspect weapons parts, now has medical and industrial

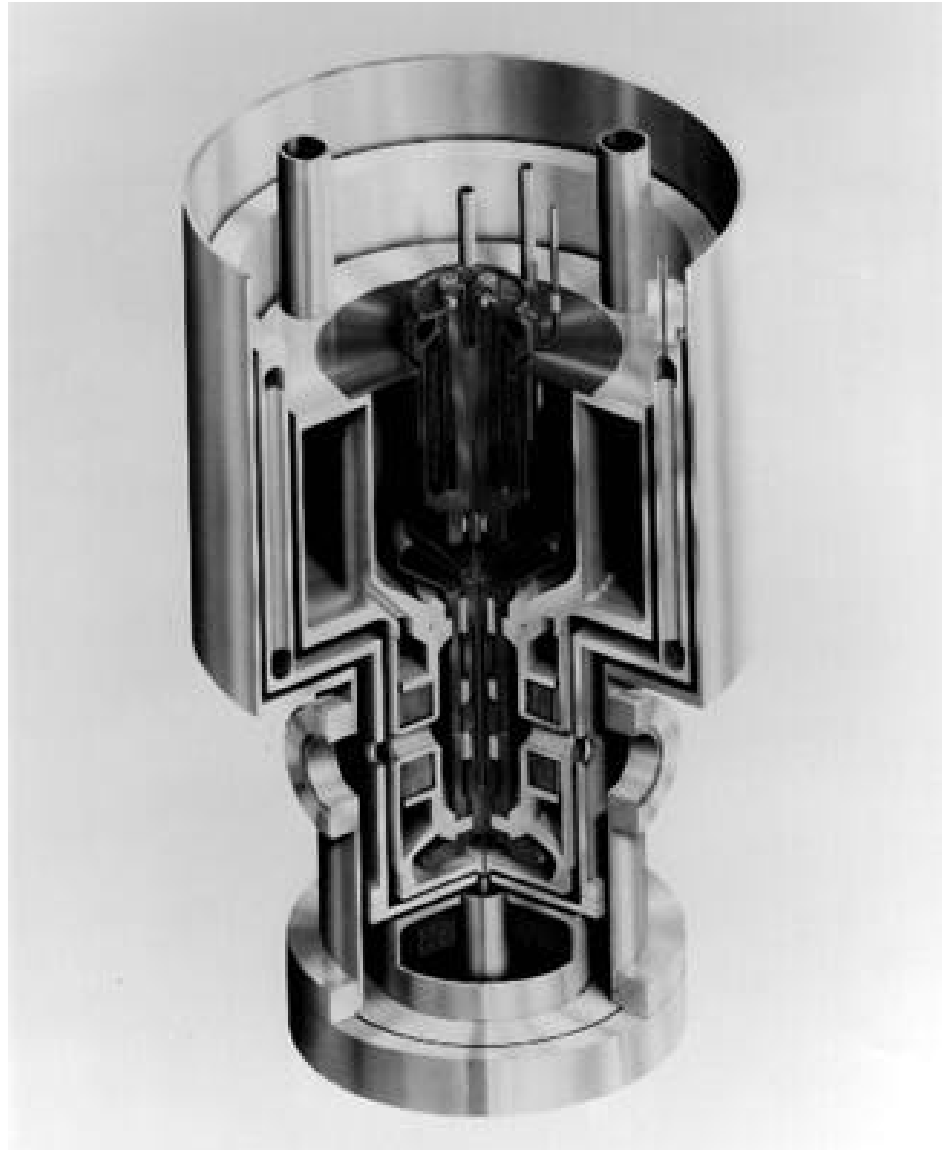


**Figure 8.** The EBIT (electron-beam ion trap), developed and built at LLNL to obtain direct measurements on highly charged ions. With this device, we can create very highly charged ions (up to a +82 charge state, for neon-like uranium) and then measure the x rays produced by the ions when they interact with the free electrons of EBIT's electron beam. These measurements provide data, which when compared with theoretical predictions, allow us to extend our understanding of the nature of matter.

applications. The basic technique involves illuminating a sample with a collimated monochromatic x-ray source to create a two-dimensional image. By using x-rays between 5 and 35 keV and rotating the sample in small angular increments through 180 degrees, we obtain enough data to reconstruct a three-dimensional image of the sample with 2- to 3- $\mu\text{m}$  resolution. This technology is similar to the CT (or CAT) scan done at a hospital, but it has a much higher resolution. It is being used to look for pores in ceramic composites, to identify potential fatigue areas in tensile loading of aircraft wings, and to study the demineralization of dentin, which leads to tooth decay.

A continuum x-ray gauging technique has been developed for nondestructive elemental analysis of materials with known constituents. For many applications, the

quantitative distribution of the components must be known. By measuring the transmission of photons at different energies, the abundance of different components can be mapped.

### X-Ray Image Enhancement

As an outgrowth of our radiography activities, we are developing a superior mammographic technique that may increase the early detection of breast cancer. Breast cancer is an important national health problem. In the United States, it kills 45,000 women each year, and the incidence of new cases increases annually, even when corrected for our aging population. To help mammographers screen the large number of mammograms, we developed a computer algorithm to locate microcalcifications in digitized mammograms. This improvement and

others will help doctors detect breast cancer at an early stage, when treatment is more successful, and thus increase the survival rate.

Breast x-ray imaging, or mammography, in combination with physical examinations, is the most effective means for detecting breast cancer at an early stage. Mammography is the only method to detect microcalcifications, which often accompany breast cancer before it is palpable—that is, when the cancer is too small to feel in a physical exam. Because microcalcifications absorb x rays more strongly than soft tissue, they are visible in a transmission x-ray image.

To detect these microcalcifications, mammographers must systematically search the traditional x-ray film using a magnifying glass. This task is tedious, time consuming, and subject to errors caused by fatigue or distraction.

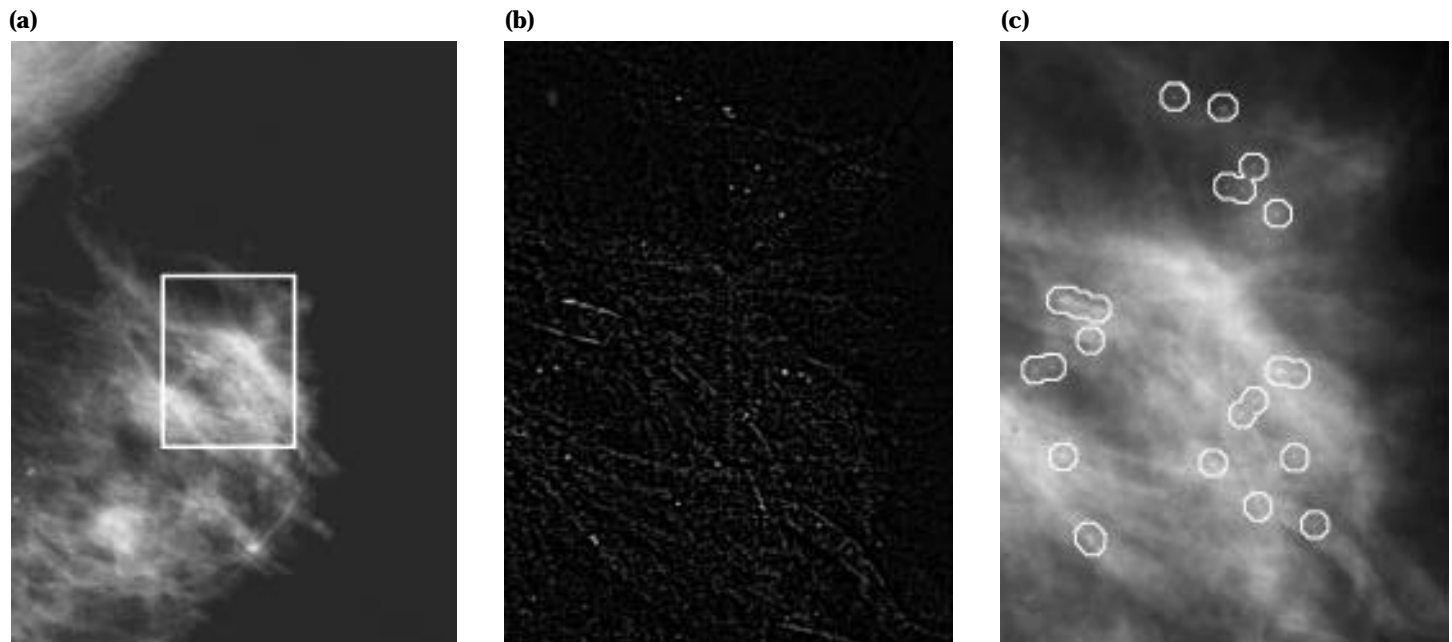


**Figure 9.** (a) A digitized mammogram. For reference, part of the pectoral muscle is visible at top left. (b) High-frequency image of the same breast—the area bordered by a rectangle in (a)—with the soft-tissue structure absent. This image was obtained after applying our algorithm. With data displayed in this manner, the pattern of calcification is evident without any distracting background information. (c) Using part of the original digital image bordered by the rectangle in (a) as background, we can highlight the most suspicious microcalcifications with circles. A mammographer can focus on the circles in the context of the overall breast structure.

“Missed” malignancies are relatively common. For example, one study found that in 320 cases of breast cancer, 77 cancers (24%) were missed by screening mammography.

The quantitative radiography techniques developed at LLNL use a computer algorithm to locate microcalcifications in digitized mammograms. **Figure 9** shows an example of a digitized x-ray mammogram. The calcifications identified by the computer program are highlighted with circles. Our computational approach can best be thought of as a “mammographer’s associate,” because it objectively and reproducibly detects and flags microcalcifications for the mammographer. This work may free mammographers from the routine and tedious search task, thus allowing them to concentrate on diagnosis.

## Conclusion

The world has changed dramatically during the last decade, and the part of the X-Ray Laser Program that President Reagan proposed is no longer being pursued.

But the decade of work on x-ray lasers has produced a rich and important legacy that includes a better understanding by physicists of x-ray lasers; sophisticated computational tools for modeling plasma physics; a laboratory x-ray laser for biological imaging; advanced materials, such as aerogel and SEAgel; unique, world-class facilities like EBIT for performing atomic physics experiments; and a superior mammographic technique for early detection of breast cancer. During the last decade, hundreds of people have participated in these efforts and helped to reshape LLNL. Their achievements have made LLNL a world leader in many fields of science and technology.

One of the newest and most sophisticated uses of x-ray lasers is as a probe for studying large, high-density plasmas. In an upcoming issue of *Energy and Technology Review*, we will describe several diagnostic techniques being developed by LLNL researchers. Our techniques include plasma imaging and, most recently, interferometry, which directly measures electron density in plasmas of the sort created by the Nova laser.

**Key words:** Aerogels—SEAgel, silica, organic; biological imaging; digital mammography; laboratory x-ray laser; multilayer mirrors; three-dimensional x-ray computer tomography; x-ray diagnostic techniques—electro-optics devices; x-ray gauging technique; x-ray laser microscopes; x-ray laser physics—electron-beam ion trap (EBIT); Strategic Defense Initiative (SDI).

## Reference

1. Technical descriptions of and related references on the research described in this article are given in Joseph Nilsen’s *Legacy of the X-Ray Laser Program*, Lawrence Livermore National Laboratory, UCRL-LR-114552 (1993).



*For further information contact Joseph Nilsen (510) 422-4766.*

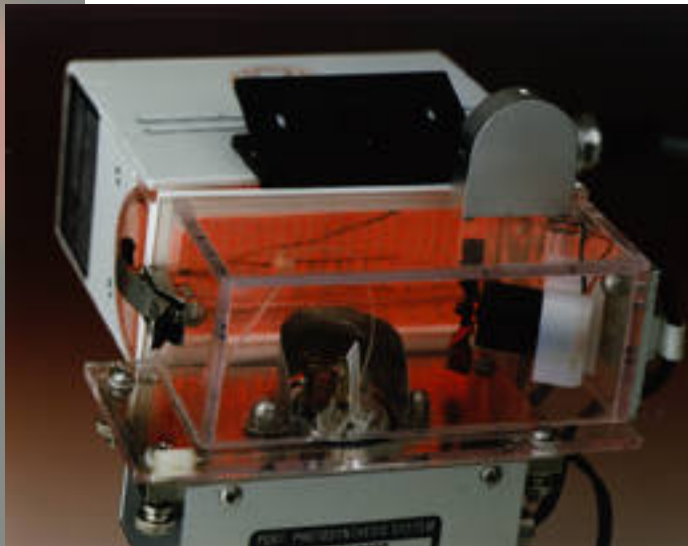
# Elevated CO<sub>2</sub> Exposure and Tree Growth

**T**HE global average climate has been relatively stable for several thousand years. However, human activities in the industrial and developing nations now threaten to cause unprecedented, rapid, and persistent climatic changes due, in large part, to changes in the composition of the Earth's atmosphere. For example, the burning of coal, oil, gas, and forests have increased the atmospheric concentration of carbon dioxide (CO<sub>2</sub>) by 25% since preindustrial times. Over approximately the same period, global average temperatures have increased by about 0.5°C, suggesting an enhanced greenhouse effect. Greenhouse gases in the atmosphere act to trap the Earth's long-wave or infrared radiation, raising the Earth's average surface temperature.

Current global atmospheric and climate models show important disagreements in their predictions. Nevertheless, projected increases in CO<sub>2</sub> (atmospheric levels are expected to double in the next century) and associated climate changes (such as warming and increased water vapor in the atmosphere) could substantially affect forests around the world. Because it is not practical to test the response of all forest habitats and species to elevated CO<sub>2</sub>, we are investigating two diverse forest species so that we can develop broad generalizations.

To assess the differential and variable effects of elevated CO<sub>2</sub> within the forest, we chose two important species of conifer, *Taxus brevifolia* and *Pinus ponderosa*. These two conifers have pronounced differences in morphology and physiology. *P. ponderosa* is an economically important, shade-intolerant, canopy-dominant conifer with a range extending from the

*Photosynthetic measuring system. This apparatus, which contains red light-emitting diodes (LEDs) as a cool source of light, is used to measure CO<sub>2</sub> uptake by a leaf. At left is a close-up view of the needles with the LEDs shown in the background.*



California coast to the Rocky Mountains and from Canada to Mexico. Climate changes affecting *P. ponderosa* could result in substantial ecological and economic impacts. *T. brevifolia*, commonly known as the Pacific Yew, is the tree from which the medicinal compound taxol is extracted. Because this conifer has higher internal limits to CO<sub>2</sub> uptake and possible limits in exporting carbon from the needles, higher levels of atmospheric CO<sub>2</sub> could be harmful to this species.

Last year, we completed the construction of an elevated CO<sub>2</sub> exposure facility at LLNL and began to gather baseline measurements. We have collected about 6000 one-year-old and four-year-old seedlings from diverse regions of California. The seedlings come from 89 genetically identified sources that can be grouped into three broad categories. In full siblings, both the male and female components are known; in half siblings, the female component is known; in open-pollinated seedlings, neither component is known.

In April 1993, we began our 3-year-long exposures of the seedlings to either ambient conditions or to elevated levels of CO<sub>2</sub> (ambient + 175 ppm CO<sub>2</sub>, or ambient + 350 ppm CO<sub>2</sub>). Multidisciplinary measurements are being collected at 3-month intervals. These measurements are giving us information on how enriched CO<sub>2</sub> affects the physiological, biochemical,

and morphological processes that are interrelated through an underlying source-sink control mechanism. As the name suggests, source-sink mechanisms in the context of our work are those that affect where a plant's carbon comes from and where the carbon ends up. For example, the principal carbon source for plants is photosynthesis, which involves the uptake and incorporation of carbon from the atmosphere. Any change in temperature or CO<sub>2</sub> will affect photosynthesis, which, in turn, affects the carbon source.

Our early results show variable growth responses in the *P. ponderosa* seedlings we have begun to assess. For example, the stem diameter of seedlings exposed to elevated CO<sub>2</sub> levels (specifically, the +350 ppm group) increased relative to the stem diameter of the ambient group, but the increases varied from 2.6% to 22.4% when these data were gathered in late 1993. On the other hand, elevated CO<sub>2</sub> resulted in a decrease in quantum yield, which is a measure of the absorption of CO<sub>2</sub> per unit of light. Once again, the responses varied among the seedling sources, ranging from -2.1% to -23.2% compared to the ambient group as of February 1994. The source trees that had the best growth throughout the study period also had the least reduction in quantum yield due to elevated CO<sub>2</sub>.

We are also measuring other physiological and biochemical changes. For example, observed decreases in the pigmentation of *P. ponderosa* due to elevated CO<sub>2</sub> are not associated with any particular family of this species. Our investigation of leaf ultrastructure, in contrast, shows differences due to family. The best growth performer shows no starch buildup in the chloroplasts, whereas the poorest growth performer shows starch buildup. (Chloroplasts are plant structures that contain chlorophyll pigments and function in photosynthesis.) The differences in starch levels were most evident during nondormant periods. Our enzymatic assays are showing that those families of seedlings with better growth at higher levels of CO<sub>2</sub> also had higher enzymatic activity.

Although it is clearly too early to draw any final conclusions, our work suggests that changes in CO<sub>2</sub> levels have complex and variable effects on plant physiology and morphology, some of which arise from a genetic component (intraspecific variability). In the coming year, we will continue to expose seedlings to elevated levels of CO<sub>2</sub> and collect multidisciplinary measurements. We also plan to expand the number of enzymatic assays we will perform. We will integrate



*The elevated CO<sub>2</sub> exposure facility at LLNL is allowing us to study the differences between conifer seedlings growing under ambient conditions and those growing under elevated levels of CO<sub>2</sub>.*

these measurements through statistical models and determine which families are responding best to the elevated exposures of atmospheric CO<sub>2</sub>. Over the longer term, our work may ultimately allow us to define long-range predictive parameters that could be used in impact assessment and forest management.

---

***For further information  
contact James L. J. Houpis  
(510) 422-0606.***

*Schematic cross section of our meniscus coating device. Coating fluid is pumped through a filter and forced through an applicator tube's longitudinal slot. Fluid attaches to the substrate by capillary forces, and a thin film is entrained on the surface. The result is extremely uniform coatings on planar substrates of nearly any size.*

# Meniscus Coating

**N**EW optical coating materials and laser technologies have created a need for large optics with uniform, ultrathin coatings that are applied from liquid solutions. Such devices are used, for example, in high-power laser systems at LLNL and elsewhere. To manufacture these optics, coatings a micron in thickness or less need to be deposited with extreme uniformity—to within a few percent—across the entire clear aperture, which can be on the order of a square meter in size.

Micron- and submicron-scale films have been traditionally applied from liquid solutions by spin coating or dip coating. However, spin coating massive optics at the high rates needed to achieve a uniform film is not practical and wastes the coating fluid. Dip coating requires large volumes of expensive coating fluids and risks intercontamination of materials in a multilayer application.

We have been investigating an alternative process known as meniscus coating. (A “meniscus” is the curved free surface of a liquid near the walls of a vessel.) Although the process has had limited use in industry for several years, it has only recently been well characterized and optimized.

The figure shows the essential features of our meniscus coating process. Coating fluid from a reservoir is forced through a filter and into the ends of a slotted applicator tube. The fluid flows up out of the slot and down over the outside of the tube to drain back into the reservoir. A surface to be coated is placed a fraction of a millimeter above the applicator tube, which moves relative to the substrate. When the liquid layer atop the tube intersects the substrate, fluid attaches to the substrate surface by capillary forces. As the relative motion continues, a thin film becomes entrained on the substrate.

The fluid dynamics that control the entrained film thickness are almost identical to those for dip coating. The film thickness is proportional to the  $2/3$  power of the translation rate of the applicator (identified as  $V$  in the

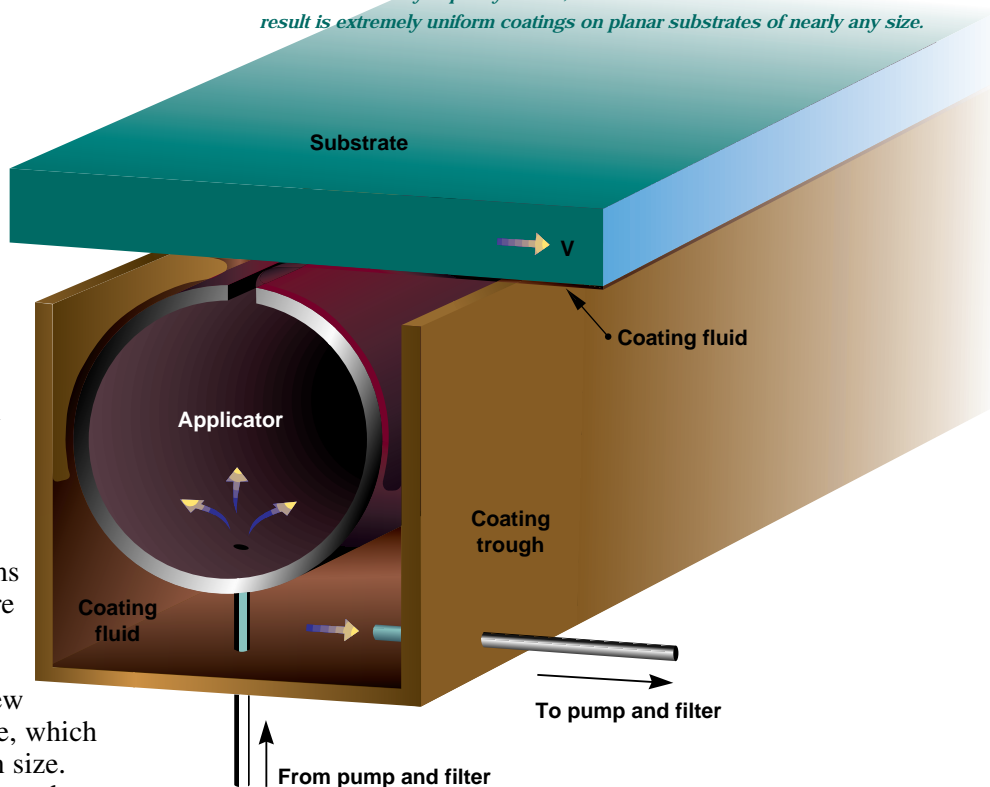


figure above). Controlling the way the film dries after it is applied is an essential step in ensuring film uniformity.

We have applied coatings 0.1 to 3.5  $\mu\text{m}$  thick and with typical uniformities of  $\pm 2.5\%$ . A distinct advantage of meniscus coating is its efficient use of the fluids. Our process provides nearly 100% utilization of a coating fluid, and with in-line filtration, its lifetime is extremely long. We have used the same 700-ml charge of fluid for over 2 months of continuous recirculation to coat dozens of substrates with no loss in performance. The process has no intrinsic scaleup limitations, so substrates of nearly any size can be coated.

One of our applications involves high reflectors (HRs) used in large-aperture, high-power laser systems. Traditional HRs are deposited by electron-beam evaporation in vacuum. Sol-gel multilayer HRs offer a low-cost, low-coating-stress alternative to traditional HRs. For example, we expect to use sol-gel HRs as cavity end mirrors for the proposed National Ignition Facility (NIF), a 192-beam megajoule-class glass laser based on a multipass amplifier architecture.

A sol-gel multilayer HR consists of alternating layers of oxide particles of high and low refractive index deposited on a substrate. Optical interference effects at the interfaces between layers cause nearly complete reflection at a desired wavelength of light, while allowing other wavelengths to be transmitted. For our application, layer thicknesses of 0.1 to 0.2  $\mu\text{m}$  are typical, and up to 30 layers are required to achieve high reflectivity in a multilayer stack.

Working with a company specializing in industrial coating machines, we have designed, built, and fielded an automated meniscus coating machine, a prototype for the machines needed to make the numerous HRs required for the NIF. The machine has been used to make a demonstration HR on the Beamlet laser, a prototype for the NIF design. This 38- × 38-cm HR contains 13 coatings of porous silica alternating with 13 layers of zirconia with a polyvinylpyrrolidone binder. The mirror has an average transmission of 1.57% with a standard deviation of 0.16%.

Large-area diffraction gratings are another important application. The technique of chirped-pulse amplification uses diffraction gratings to expand subpicosecond laser pulses in time and then to recompress them after amplification. This technique is allowing researchers to develop new laser systems that can deliver power levels of more than one terawatt ( $10^{12}$  W). Such power levels offer exciting opportunities for studying the interaction of light and matter and for investigating fusion power.

The internally funded petawatt project at LLNL will convert one of the ten beams of the Nova laser into an independent laser capable of delivering a petawatt ( $10^{15}$  W) of power in a 1-picosecond pulse. The pulse-

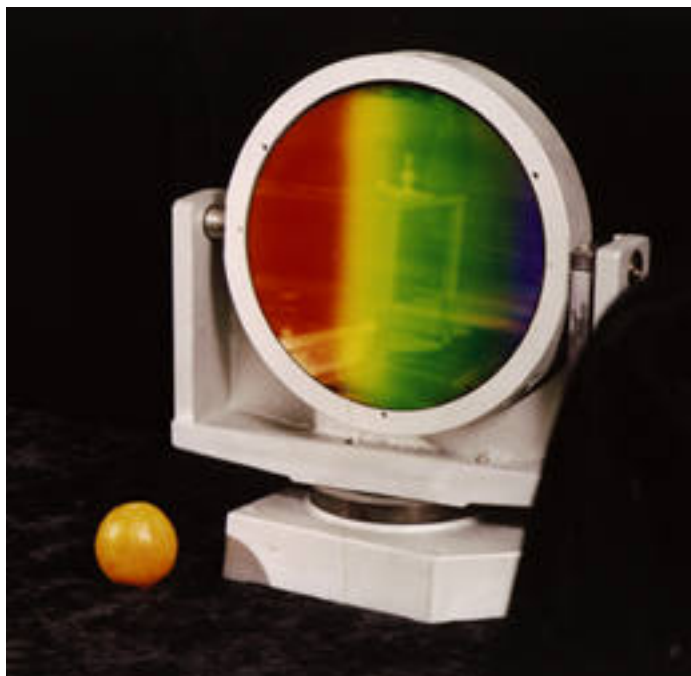
compression gratings in the Petawatt laser will be approximately  $100 \times 60$  cm in size. Gratings this large can only be made by holographic techniques. A photoresist film on the substrate is exposed to the interference pattern resulting from the intersection of two highly collimated (nearly parallel) ultraviolet laser beams, and the exposed pattern in the resist is developed. The grating structure in photoresist is then overcoated with a metal layer (usually gold) to make a high-efficiency reflective grating.

We have created high-efficiency gratings by applying the photoresist film at the thickness corresponding to the line height that maximizes grating efficiency. We then process the optic so that the exposed photoresist dissolves down to the substrate, whereas the unexposed resist remains at nearly the original film thickness.

We have used our meniscus coating procedure to make several 30-cm-diameter gratings (photo below). These gratings exhibit 94% absolute diffraction efficiency for 1.06- $\mu\text{m}$  light. We have also made several 15- and 30-cm-diameter gratings of similar quality for pulse compression of 825-nm light. Our next challenge is to make the large gratings for the Petawatt laser.

Flat panel displays are a promising new application with a huge potential market. These devices present a challenge to current processing technologies from both cost and performance standpoints. At present, their processing involves spin coating photoresist and color filter layers onto glass panels, a procedure borrowed from integrated-circuit manufacturing. Such processing is both unwieldy and expensive because the coating fluids cost several hundred dollars per liter, and about 99.5% of the applied liquid is flung off the substrate during the high-rpm process. Edge nonuniformities in film thickness are also plainly visible on large rectangular or square spin-coated glass panels.

We have demonstrated that meniscus coating can provide adequate coating uniformity and reproducibility for flat panel display processing, along with nearly 100% utilization of coating fluids. We are confident that our technology has a bright future in this new application.



*One of our new 30-cm-diameter diffraction gratings used for pulse compression of high-power lasers. This grating, with 1740 lines per millimeter, exhibits 94% absolute diffraction efficiency for 1.06- $\mu\text{m}$  light, and it has a wavefront flatness of less than one-fifth wave over the usable aperture.*

---

***For further information  
contact Jerald A. Britten  
(510) 423-7653.***

### **LLNL's 1994 R&D 100 Awards**

Each year *R&D Magazine* selects the 100 most technologically significant products and processes submitted for consideration and honors them with an R&D 100 award. The R&D 100 judges look for products or processes that promise to change people's lives, such as by significantly improving the environment, health care, or security. Since the competition began in 1963, the Laboratory has won 50 R&D 100 awards. In 1994, the Laboratory received six R&D 100 awards. Three of them—multilayer dielectric diffraction gratings, methods for rapidly growing high-quality crystals, and several varieties of apatite crystals doped with ytterbium—contribute to advances in laser technology (and in turn to research in inertial confinement fusion, which promises someday to be a major source of energy for civil uses). We have advanced the limits of high-precision metrology by developing an amplifier for use with sensors that measure surface irregularities; and to increase the speed of fiber-optic communication, we have developed a method of achieving submicrometer accuracies of component alignment at 10 to 20 times less cost than that of current methods. Finally, our chromosome-specific DNA probes for identifying chromosomes of the laboratory mouse are 60 times faster than the standard banding method. The Laboratory's six 1994 awards demonstrate once again that research derived from defense concerns can contribute civil applications that advance U.S. economic competitiveness and promise improved human well being.

**Contacts: Michael D. Perry (510) 423-4915, Robert Boyd (510) 422-6224, James De Yoreo (510) 423-4240, Stephen A. Payne (510) 423-0570, David Hopkins (510) 423-6134, Michael Pocha (520) 422-8664, and James D. Tucker (510) 423-8154.**

### **Legacy of the X-Ray Laser Program**

The X-Ray Laser Program, which evolved from a laser system that could protect against Soviet missiles, achieved many great technical and physics accomplishments. We are finding that much of the technology developed by the program can be used to advance research in weapons diagnostics, plasma physics, biotechnology, medicine, and industrial materials. The program's legacy includes: development of advanced electro-optic diagnostic devices; a better understanding of x-ray laser physics; an array of sophisticated computational tools for modeling plasma physics; a laboratory x-ray laser for biological imaging; the development of advanced materials, such as aerogel and SEAgel; new measurement techniques for characterizing materials; and a unique, world-class research facility, called the electron-beam ion trap (EBIT), for performing atomic physics experiments.

**Contact: Joseph Nilsen (510) 422-4766.**